Chem Soc Rev

Cite this: *Chem. Soc. Rev.*, 2012, **41**, 6944–6976

www.rsc.org/csr

**TUTORIAL REVIEW**

# Graphene electrochemistry: fundamental concepts through to prominent applications

**Dale A. C. Brownson, Dimitrios K. Kampouris and Craig E. Banks***

***Received 30th March 2012***
**DOI: 10.1039/c2cs35105f**

The use of graphene, a one atom thick individual planar carbon layer, has exploded in a plethora of scientific disciplines since it was reported to possess a range of unique and exclusive properties. Despite graphene being explored theoretically since the 1940s and known to exist since the 1960s, the recent burst of interest from a large proportion of scientists globally can be correlated with work by Geim and Novoselov in 2004/5, who reported the so-called ''scotch tape method'' for the production of graphene in addition to identifying its unique electronic properties which has escalated into graphene being reported to be superior in a superfluity of areas. Consequently, many are involved in the pursuit of producing new methodologies to fabricate pristine graphene on an industrial scale in order to meet the current world-wide appetite for graphene. One area which receives considerable interest is the field of electrochemistry, where graphene has been reported to be beneficial in various applications ranging from sensing through to energy storage and generation and carbon based molecular electronics. Electrochemistry is an interfacial technique which is dominated by processes that occur at the solid–liquid interface and thus with the correct understanding can be beneficially utilised to characterise the surface under investigation. In this *tutorial review* we overview fundamental concepts of Graphene Electrochemistry, making electrochemical characterisation accessible to those who are working on new methodologies to fabricate graphene, bridging the gap between materials scientists and electrochemists and also assisting those exploring graphene in electrochemical areas, or that wish to start to. An overview of the recent understanding of graphene modified electrodes is also provided, highlighting prominent applications reported in the current literature.

## 1. Introduction to graphene

The IUPAC suggested definition of graphene is: ''*a single carbon layer of the graphite structure, describing its nature by analogy to a polycyclic aromatic hydrocarbon of quasi infinite size*''.[1] It is then noted that *''previously, descriptions such as graphite layers, carbon layers or carbon sheets have been used for the term graphene. Because graphite designates that modification of the chemical element carbon, in which planar sheets of carbon atoms, each atom bound to three neighbours in a honeycomb-like structure, are stacked in a three-dimensional regular order, it is not correct to use for a single layer a term which includes the term graphite, which would imply a three-dimensional structure. The term graphene should be used only when the reactions, structural relations or other properties of individual layers are discussed''*.[1] Clearly inspection of the current literature would then mean that a considerable number of publications are re-classified! The exact history of graphene and how it appeared on the scientific horizon is compelling, with the 2010 Nobel Prize in Physics awarded for ''*ground-breaking experiments regarding the two-dimensional material graphene*''.[2] Indeed, in 2004 Geim and Novoselov developed a very simple methodology (the so called ''scotch tape'' approach) which allowed them to produce and observe microscopic few-layer graphene on oxidised silicon wafers, which was copied globally as a protocol to produce large area single layer graphene samples for two-dimensional transport studies.[3] However as noted by de Heer,[4] the majority of papers incorrectly cite the 2004 paper by Novoselov and Geim as the paper that presented both the 'scotch tape method' and graphene's unique electronic properties to the world. In fact such findings were not reported with regards to individual single layer graphene in 2004[3] but actually in 2005.[4,5] Furthermore, in truth, graphene had been identified and characterised as a two-dimensional-crystalline material in many reports prior to 2004 where ultra-thin graphitic films were observed and occasionally even monolayer graphene (see for example ref. 6 for reviews). Interestingly however, these prior reports

*Faculty of Science and Engineering, School of Science and the Environment, Division of Chemistry and Environmental Science, Manchester Metropolitan University, Chester Street, Manchester M1 5GD, Lancs, UK. E-mail: c.banks@mmu.ac.uk; Web: www.craigbanksresearch.com; Fax: +44 (0)1612476831; Tel: +44 (0)1612471196*

were merely observational and failed to describe any of graphene's distinguishing properties; thus the 2005 report by Novoselov and Geim can be considered as the first to report both the isolation of 'pristine' graphene (*i.e.* single layer graphene without heteroatomic contamination) and its unique properties, which in doing so sparked the graphene gold rush and brought new and exciting physics to light.[6] Since the pioneering reports of 2004/5 many other unique properties have been assigned to graphene, such as having a high optical transparency of 97.7%, high electron mobility of up to 200 000 $cm^2\ V^{-1}\ s^{-1}$, high thermal conductivity of up to 5000 $W\ m^{-1}\ K^{-1}$, a high nominal surface area of 2630 $m^2\ g^{-1}$, and a high breaking strength of 42 $N\ m^{-1}$.[7–10] From this point onwards, graphene has captured the imagination of scientists and is now a hugely active area of research in a plethora of fields, none more so than in the field of electrochemistry which has reported many benefits in the areas of sensing through to energy storage and generation.

This tutorial review first provides a brief introduction into electrochemistry which allows recent key developments in the field of Graphene Electrochemistry to be understood. The review makes this field accessible to other scientists working with graphene such that they can apply electrochemistry as a characterisation tool and it also provides an introduction to those starting work in the field of *Graphene Electrochemistry*. Before considering graphene, it is insightful to first overview graphite surfaces where a significant amount of information has been gathered over many decades.

Graphite surfaces are heterogeneous (anisotropic) in nature, with the overall chemical and electrochemical reactivity differing greatly between two distinct structural contributions which are fundamental to the behaviour of graphitic electrodes, namely the edge and basal planes.[11] Fig. 1 depicts a schematic representation of a surface of Highly Ordered Pyrolytic Graphite (HOPG) showing discrete edge plane and basal plane islands and a side on view highlighting the edge plane and basal plane like-sites/defects which exhibit contrasting electrochemical behaviour, where electrochemical reactions on the former have been shown to be anomalously fast over that of the latter.[12–14] Note that under certain (limited) conditions the basal plane sites have measurable electrochemical activity.[15] Recently it has been shown *via* Scanning Electrochemical Cell Microscopy (SECM) that the basal plane sites of *freshly exposed* HOPG display considerable electroactivity which, interestingly, is time dependant, in that exposure to air for less than one hour after cleaving leads to a decrease in the observed electron transfer rates at the basal surface.[15c] Such work is highly fascinating and studies into this time-dependent surface effect are, at the time of writing this review, underway,[15c] but ultimately this means that over the lifetime of an experiment the observed electroactivity of the freshly cleaved basal plane sites of HOPG becomes negligible as previously reported.[12–14]

**Dale A. C. Brownson**

*Dale A. C. Brownson received his BSc (H) in Forensic Science with Criminology from Manchester Metropolitan University in 2010 and is currently commencing the final year of his PhD in Chemistry at the same university. His PhD is focussed on expanding the horizons of graphene electrochemistry, which encompasses the exploration of fundamental understanding in addition to applications in sensing and energy related devices. Dale has published over 18 papers with a h-index of 7 (Web of Science, June 2012) and has also written 1 book and contributed 2 book chapters. Other research interests include forensic applications of chemistry, with particular focus on analytical techniques.*

**Dimitrios K. Kampouris**

*Dimitrios K. Kampouris is currently a postdoctoral research associate at Manchester Metropolitan University, working in collaboration with Kanichi Ltd. He received his PhD in Chemistry from Manchester Metropolitan University in 2010 with a thesis focused on the development of materials for electrochemical applications. Dimitrios has published 24 papers with a h-index of 8 (Web of Science, June 2012) and is the inventor of 7 patents. His interests are in carbon materials and their application in electrochemistry, including use in energy storage and as advanced materials in electroanalysis. Other research interests include the synthesis of nanomaterials, particularly the application of screen and inkjet printing towards the production of nano-devices.*

**Craig E. Banks**

*Craig E. Banks is an Associate Professor of Chemistry at Manchester Metropolitan University and has published over 200 papers with a h-index over 37 (Web of Science, June 2012). He has written 4 books, contributed 10 book chapters and is an inventor of 13 patents. Craig has also spun out two companies from his research. Craig was awarded the Harrison–Meldola Memorial Prize in 2011 for his contributions to the understanding of carbon materials, in particular graphene and its application as an electrode material. His current research is directed towards the pursuit of studying the fundamental understanding and applications of nano-electrochemical systems such as graphene, carbon nanotube and nanoparticle derived sensors and developing novel electrochemical sensors via screen printing and related techniques.*

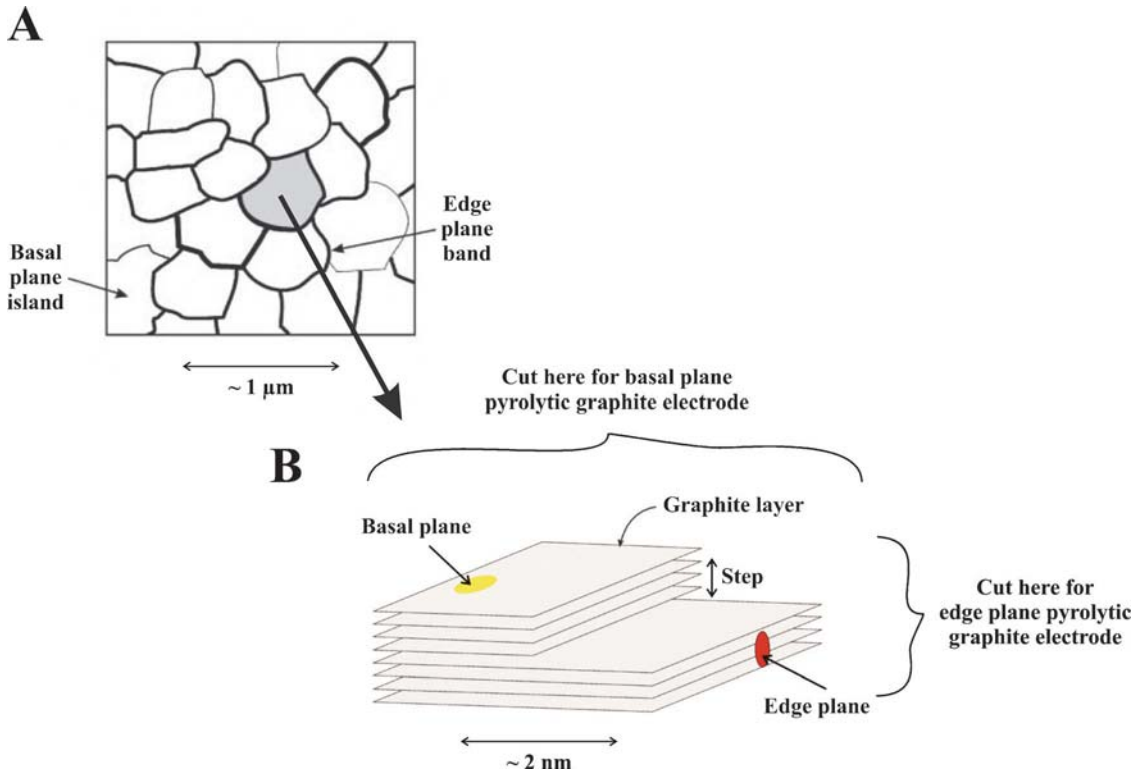


**Fig. 1** A: Schematic representation of a HOPG surface showing discrete basal plane and edge plane islands. B: Side on view of the HOPG surface highlighting its basal plane and edge plane like-sites/defects which exhibit contrasting behaviours in terms of electrochemical activity, where electron transfer kinetics of the latter are overwhelmingly dominant over that of the former which in comparison are relatively (electrochemically) inert.[12–14] Figure adapted from ref. 14 with permission of The Royal Society of Chemistry.

The structural characteristics of graphitic materials relate to the intraplanar microcrystallic size, $L_a$ and interplanar size, $L_c$ which is shown schematically in Fig. 2 for the case of HOPG and graphene. It is evident in terms of the intra-/inter-planar characteristics, $L_a$ and $L_c$, that "a" refers to the atomically ordered hexagonal plane, known as the *basal plane* while the irregular surface "c" is termed the *edge plane*. Also shown in Fig. 2 is the range of $L_a$ and $L_c$ values for a collection of other graphitic forms where it is evident that HOPG has $L_a$ and $L_c$ values exceeding 1 μm while polycrystalline graphite has values from 10 to 100 nm and carbon black from 1 to 10 nm. Graphene that is readily obtainable from a range of commercial suppliers is also included, highlighting the variation in structure that can be obtained, which is of course dependant on the fabrication methodology; $L_a$ values for graphene can range from below 50 up to 3000 nm and larger, and of course true (monolayer) graphene possess an $L_c$ value of 0.35 nm.

An important parameter of an electrode material is its electronic properties, namely, the Density Of electronic States (DOS) which varies greatly on the different forms of graphite. Gold typically has a DOS of 0.28 states atom$^{-1}$ eV$^{-1}$ with the high conductivity of gold arising from the combination of a high proportion of atomic orbitals to form bands with a high density of electronic states.[11] For a given electrode material, a higher DOS increases the possibility that an electron of the correct energy is available for the electrode to transfer to an electroactive species; the heterogeneous electron transfer rate is thus dependent on the DOS of the electrode material.[11] HOPG has a DOS which overall is lower than that of metal, but is particularly low near the Fermi level and has been reported to have a minimum DOS of around 0.0022 states atom$^{-1}$ eV$^{-1}$, which is about 0.8% that of gold.[11]

The DOS at graphitic materials can be increased through disorder such that electroactive species exhibit increasing electron transfer rates but by varying amounts; in terms of outer-sphere electron transfer systems, disorder increases the rate by modifying the electronic structure of the carbon while for inner-sphere systems, specific surface interactions also contribute (see later).[16] A perfect/pristine basal surface of HOPG has no edge plane (in theory), no location for surface functional groups and there are no dangling bonds since the carbon atoms have satisfied valances.[11] When disorder is introduced, such as through mechanical roughening of the electrode surface, the surface is disturbed such that surface defects are introduced, *viz* edge plane sites which increase the DOS.[11] A further extreme is the complete change of a graphitic surface to a different structural composition ($L_a$ and $L_c$; see Fig. 2) towards that of Edge Plane Pyrolytic Graphite (EPPG) which has a high proportion of edge plane sites and thus improvements in electron transfer are observed.[11]

Electronic properties of graphitic materials are thus highly relevant and critical, where the energy-dependant densities of electronic states have major effects on electron transfer. Note that graphitic materials differ greatly in their surface chemistry which is also critical when understanding electrochemical processes at these materials.[11] Such insights from graphitic

 

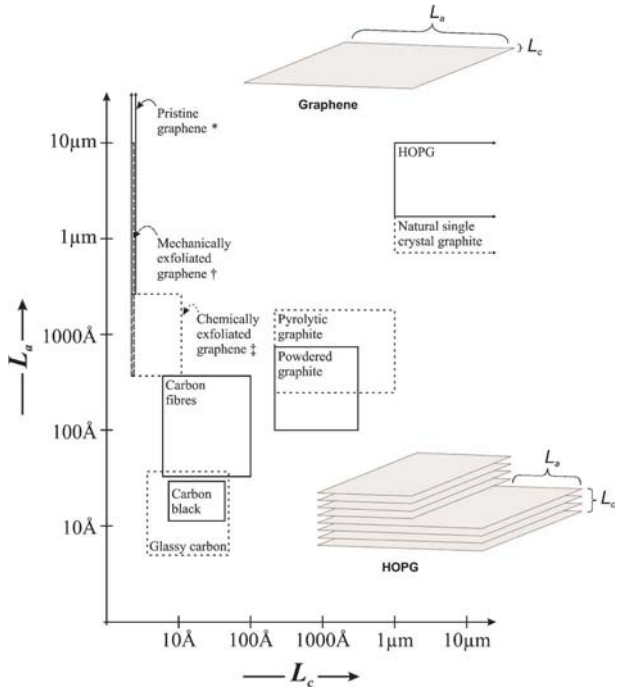


**Fig. 2** The approximate ranges of $L_a$ and $L_c$ values for various $sp^2$ carbon materials. Note, there is large variation of $L_a$ and $L_c$ with sample history and thus the values shown should be considered representative, yet approximate. *: Pristine graphene; commercially available from 'Graphene Supermarket', produced *via* a substrate-free gas-phase synthesis method.[30,31] ‡: Chemically exfoliated graphene; commercially available from 'NanoIntegris', produced *via* a surfactant intercalation process – note that this range is also representative of graphene produced through other chemical exfoliation routes such as the reduction of GO.[27,28] †: Mechanically exfoliated graphene was fabricated through the so-called 'scotch tape method'. Note that graphene synthesised *via* CVD has been excluded given that crystal size and quality are large variables through this route, however single graphene crystals with dimensions of up to 0.5 mm have been reported.[34,37] A schematic representation of the $L_a$ and $L_c$ microcrystalline characteristics of graphene and HOPG is also shown.

materials can be applied for the case of graphene. In terms of the DOS for graphene, insights from HOPG can be illuminating to understand its electrochemical reactivity. For a diffusional outer-sphere electron transfer process, the standard electrochemical rate constant, $k^o$, can be defined as:[17,18]

$$k^o = \frac{(2\pi)^2 \rho H_{DA}^{o\,2}}{\beta h\sqrt{4\pi\Lambda}} \exp\left[-\frac{\Lambda}{4}\right] I(\theta,\Lambda) \qquad (1)$$

where $\rho$ is the density of electronic states in the electrode material, $H_{DA}^o$ is the electronic coupling matrix at the closest distance of approach, $\Lambda = (F/RT)\lambda$, where $\lambda$ is the reorganisation energy, $\beta$ is its associated electronic coupling attenuation coefficient, $h$ is Planck's constant, $F$ is the Faraday constant (96 485 C $mol^{-1}$), $R$ the gas constant (8.314 J $mol^{-1}$ $K^{-1}$) and $T$ the absolute temperature (K). $I(\theta, \Lambda)$ is an integral give by:[18]

$$I(\theta,\Lambda) = \int_{-\infty}^{\infty} \frac{\exp[-(\varepsilon-\theta)^2/4\Lambda]}{2\cosh[\varepsilon/2]} d\varepsilon \qquad (2)$$

where $\theta = F/RT(E - E_f^0)$, and $E_f^0$ is the formal potential. Thus from inspection of eqn (1) there is a direct relationship between the DOS and the standard electrochemical rate constant ($k^o$). Thus this can be interpreted for graphite as the DOS varies significantly as a function of energy with a minimum at the Fermi level.[18] It has been shown that electron transfer is non-adiabatic and the rate of electron transfer varies as a function of the applied potential as is evident from inspection of eqn (1).[18]

It has been reported that the basal plane of pristine graphene has a DOS of 0 at the Fermi level, which was shown to increase with edge plane defects.[19,20] Conversely the edge plane sites on graphene nanoribbon's zigzag edge have been reported to possess a high DOS.[20] Other work has shown that depending on how the edge of graphene terminates,[21] a variable DOS is observed.[22] Thus, graphene, a single layer comprising HOPG, should in theory act similar in terms of its DOS to that observed for HOPG (see above); that is, pristine graphene with no defects should exhibit poor electrochemical behaviour and on the contrary graphene possessing a high degree of defects should exhibit improvements in the observed electrochemical rate constant.

There is a wealth of literature on graphene which reports that the edge of graphene is particularly more reactive than its side (basal plane). For example, using Raman spectroscopy Strano and co-workers[23] report the reactivity of graphene, that being single-, double-, few- and multi-layer towards electron transfer chemistries with 4-nitrobenzenediazonium tetrafluoroborate. Strano *et al.*[23] interpret their observations with consideration to the Gerischer–Marcus theory which states that the charge transfer depends on the electronic DOS of the reacting species and is not restricted to their Fermi levels only. The observed electron-transfer reaction rate ($k_{Graphene}^{OBS}$) is given by eqn (3) where $W_{OX}(\lambda,E)$ is the distribution of the unoccupied redox states of the electron acceptor in solution given by eqn (4). The $DOS_{Graphene(N=1/N=2)}$ is the electronic density of states of graphene for $N = 1$, and of double layer graphene for $N = 2$ and $\varepsilon_{OX}$ is the proportionality function.[23]

$$k_{Graphene}^{OBS} = \nu_n \int_{E_{redox}}^{E_F^{Graphene}} \varepsilon_{OX}(E) DOS_{Graphene(N=1/N=2)}(E) \times W_{OX}(\lambda,E) dE \qquad (3)$$

$$W_{OX}(\lambda,E) = \frac{1}{\sqrt{4\pi\lambda kT}} \exp\left(-\frac{(\lambda-(E-E_{redox}))^2}{4\lambda kT}\right) \qquad (4)$$

Calculations presented by Strano *et al.* suggest that double layer graphene is almost 1.6 times more reactive than single layer graphene.[23] Thus based on the DOS, it is clear that double layer graphene is more reactive than single layer graphene, which has clear implications for graphene as an electrode material; it is this we explore later in this tutorial review in more detail.

### 1.1. Fabricating graphene

Preparative methods of graphene are currently a heavily researched and important issue. The search for a methodology that can reproducibly generate high quality monolayer graphene

sheets with large surface areas and large production volumes is greatly sought-after. Consequently, several physical and chemical methods exist for the production of graphene, which include the mechanical or chemical exfoliation of graphite, unrolling of Carbon Nanotubes (CNTs) (either through electrochemical, chemical or physical methods), Chemical Vapour Deposition (CVD) or epitaxial growth, reduction of Graphene Oxide (GO) and many other organic synthetic protocols.[7–9,24,25] It is important to note however that each method has innate advantages and disadvantages in terms of the resultant quality (properties), quantity and thus electrochemical applicability of the graphene produced and that there is presently no single method that exists for the production of graphene sheets that are suitable for all potential applications.[7,9]

Among the methods stated above, dry mechanical exfoliation remains one of the most popular and successful methods for producing single or few layers of graphene.[26] The method involves cleaving a sample of graphite (usually HOPG) with a cellophane-based adhesive tape.[3] The number of graphene layers formed can be controlled to a limited degree *via* the number of repeated peeling steps before the flakes can then be transferred to appropriate surfaces for further study. This method is ideally suited for the investigation of graphene's physical properties given that it allows the low cost isolation of single graphene sheets that are of high quality,[3,24] however, disadvantages including poor reproducibility, low-yield and the labour intensive processes required result in it being difficult to scale this process to mass production and have thus lead to this method being used predominantly only for fundamental studies.[24] Furthermore, possible damage (disrupting the basal surface, *viz* the generation of edge plane like-sites/defects) and contamination of the graphene samples, particularly from the adhesive utilised in the cellophane-based tape, renders this method less appealing for the electrochemical investigation of pristine graphene.

An alternative preparative method that is commonly utilised owing to the ease of production, high-yield and relative low cost is the chemical exfoliation of graphite.[24] This includes ultrasound in both solution and intercalation steps, usually prior to the implementation of a centrifugation technique. For example, one ultrasonication route entails the use of a water-surfactant solution, sodium cholate,[27] which forms stable encapsulation layers on each side of the graphene sheets; graphite flakes are dispersed in the aqueous surfactant solution and transformed into monolayer graphene by the application of ultrasound, resulting in graphene–surfactant complexes having buoyant densities that vary with graphene thickness.[27] Following sonication the obtained solutions undergo centrifugation, which results in a 'sorting' of the graphene and hence different fractions are observed meaning that graphite and multi-layer graphene are not inadvertently incorporated into the graphene samples, after which the upper part of the resultant supernatant contains single layers of graphene floating in the solution which are then transferred using a pipette and dropped onto the surface of choice for further study.[27] Note that graphene fabricated *via* this route is readily commercially available.[27,28] This procedure is also possible without additives in many organic solvents that have a high affinity for graphite where ultrasonic agitation is used to supply the energy to cleave the graphene precursor.[29] The success of ultrasonic cleavage depends on the correct choice of solvents and surfactants as well as the sonication frequency, amplitude and time.[29] Note that as with mechanical exfoliation, the quality of the obtained graphene is not always sufficient (structural damage to the graphene can occur during preparation owing to ultrasonication, which may result in the graphene possessing a high density of defects) and additionally homogeneity of the number of graphene layers is often poor,[24] thus graphitic impurities may remain. Note also that material produced *via* such means often contains remains from the exfoliating agents utilised. These impurities can significantly affect the observed electrochemical characteristics and performance of the graphene sample (see later for further details – Sections 2.3.2 and 2.3.3).

Note that recent developments have led to the commercial availability of 'pristine' graphene that is produced *via* a substrate-free gas-phase synthesis method.[30,31] This single-step technique involves sending an aerosol consisting of liquid ethanol droplets and argon gas directly into a microwave-generated argon plasma (at atmospheric-pressure), where over a time scale in the order of $10^{-1}$ s, ethanol droplets evaporate and dissociate in the plasma forming solid matter that through characterisation by Transmission Electron Microscopy (TEM) and Raman spectroscopy is confirmed to be clean and highly ordered graphene sheets that are similar in quality to the graphene obtained through the mechanical exfoliation of HOPG.[30,31] When commercially available, the fabricated graphene sheets are sonicated in ethanol to form a homogeneous suspension before being distributed by the supplier.[31] Production in this manner has proven that graphene can be created without the use of three-dimensional materials as precursors or supporting substrates, and has demonstrated the viability of the large-scale synthesis of graphene.

Another popular aqueous based synthetic route for the production of graphene utilises GO.[9,24] GO is produced *via* *graphite* oxide which itself can be fabricated *via* various different routes. The Hummers method for example involves soaking graphite in a solution of sulphuric acid and potassium permanganate to produce graphite oxide.[24,32] Stirring or sonication of the graphite oxide is then performed to obtain single layers of GO – this is achieved given that GO's functional groups render it hydrophilic, allowing it to be dispersed in water based solutions. Finally, GO is chemically, thermally or electrochemically reduced to yield graphene.[8,24] Note that the majority of graphene used in electrochemistry is produced through the reduction of GO (often referred to as 'reduced GO' or 'chemically modified graphene'), it is important to note that graphene produced in this manner usually has abundant structural defects (edge plane like-sites/defects)[25,33] and remaining functional groups which results in partially functionalised graphene and thus is not pristine graphene: this has implications with regards to contributory factors influencing the observed electrochemistry (see later). This method has the advantages of being scalable, rapid and cost effective in addition to the beneficial handling versatility of the liquid suspension;[7] however, (as stated above) reduction to graphene is often only partial, lattice defects and graphitic impurities

 

can also remain after reduction and additional interferences may arise in this case from the presence of reducing agents.

Note that the more practical solution-chemistry based approaches towards the fabrication of graphene are currently favoured for electrochemical applications because of their high yields and the flexibility of handing the graphene obtained from these processes.[26] In these cases the graphene is usually dispersed into a solvent which is then cast onto a suitable surface, where following evaporation the graphene left immobilised can then be used experimentally. This process, while facile, has inherent disadvantages such as surface instability, reproducibility and uncertainty issues in terms of the coverage and quality of the graphene remaining where deviation from true single layer 'pristine graphene' may exist (*viz* graphitic impurities) and as a consequence in these instances post-application characterisation of the graphene is required for clarity.[7] Yet it is an effective way to explore the electrochemical properties of graphene.

One interesting fabrication approach is the CVD growth of graphene. This method appears ideally suited for applications within electrochemistry with regards to the prevalence of uniform graphene sheets with high crystal quality and large surface areas, which are readily transferable and can be obtained at large manufacturing volumes.[34,35] Additionally, CVD fabricated graphene is often supported on a (desirable and suitable) solid substrate and as such the positioning and orientation of the graphene can be precisely manipulated for specific purposes, alleviating issues with regards to the controlled placement of solution based graphene sheets and in terms of the natural formation of graphite once the solvent is removed, as has been reported in some cases.[34] The underlying principle of CVD is to decompose a carbon feedstock with the help of heat in order to provide a source of carbon which can then rearrange to form $sp^2$ carbon species. This is usually accomplished over a catalyst;[24] for the growth of graphene, hydrocarbon gases are generally utilised as precursors and the most successful catalysts thus far are transition metal surfaces (namely nickel and copper).[36] In recent groundbreaking work, single graphene crystals with dimensions of up to 0.5 mm were grown by low-pressure CVD in copper-foil enclosures using methane as a precursor.[37] Low-energy electron microscopy analysis showed that the large graphene domains had a single crystallographic orientation, with an occasional domain having two orientations.[37] The authors report that Raman spectroscopy revealed the graphene crystals to be uniform monolayer's with a low D-band intensity.[37] Scanning Electron Microscope (SEM) images of the fabricated graphene are presented in Fig. 3 – this work was the first to report the growth of high quality large-grain-size *single* graphene crystals. However, bear in mind that recent studies of graphene produced by CVD on copper (and particularly on nickel)[34] showed that the majority of graphene produced is few- and multi-layered, in addition to being polycrystalline where its resultant mechanical strength is weakened (and its electronic properties altered) at the grain boundaries of the underlying substrate, which are the origin of surface defects in graphene (graphitic impurities) and thus in an electrochemical sense the degree of defect coverage will strongly influence the electrochemical properties of the graphene film (see later).

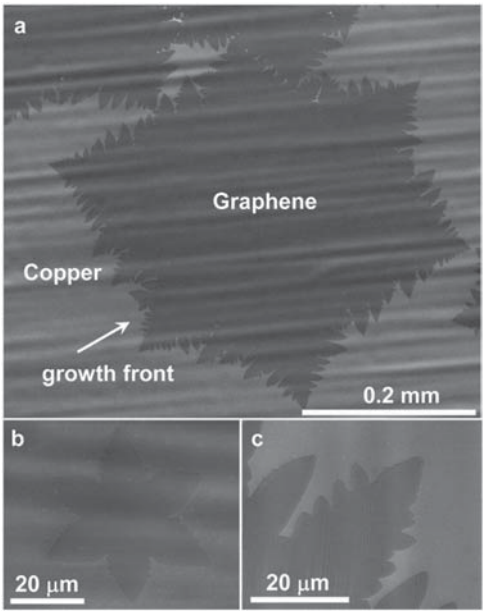


**Fig. 3** SEM images of graphene on copper grown by CVD. (a) Graphene domain grown at 1035 °C on copper at an average growth rate of ~6 μm $min^{-1}$. (b) Graphene nuclei formed during the initial stage of growth. (c) High-surface-energy graphene growth front shown by the arrow in (a). Reprinted with permission from ref. 37. Copyright 2011 American Chemical Society.

Furthermore, note that for the case of the CVD fabrication of CNTs, metallic impurities are commonly the 'hidden' origin of electrochemical activity for many analytes, which is inherent to the CVD fabrication process, where the amount of metallic impurities varies greatly between batches and hinders exploitation, for example in the fabrication of reliable CNT based sensor and energy devices.[38] It is clear that where graphene is fabricated *via* CVD appropriate control experiments will need to be performed in order to confirm the absence of such metallic impurities. Additionally, given the possible contribution of the underlying metal support/catalyst towards the observed electrochemistry at CVD grown graphene (where incomplete coverage of the graphene layer occurs – see Section 2.3.7), investigations towards the utilisation of non-metallic catalysts for graphene's CVD synthesis are also encouraged to overcome this potential issue. Note that alternatively, transfer of the fabricated graphene onto a more suitable insulating substrate is often necessary, and whilst it is possible,[39] transferring graphene to these substrates is not so straight forward and damage to the graphene can occur and thus more efficient processes need to be developed.[34]

With future work in this field focusing on the use of single crystal substrates for the CVD growth of graphene, through careful control of the experimental conditions one can envisage high quality, contaminant free, single layered graphene crystals of bespoke sizes with controllable orientation and defect density (or alternatively selectively impure graphene with customised properties, see later)[34] being made commercially available within the near future – all of which are beneficial for the electrochemical utilisation of graphene. It is however important to note; given that the structural characteristics and/or composition of graphene vary significantly depending

on the fabrication route utilised, it is essential that any such fabricated graphene nanomaterial is thoroughly characterised prior to its implementation within electrochemistry to avoid potential misinterpretation of the experimental data.

## 2. The electrochemistry of graphene

### 2.1. Introduction to electrochemistry

It is well established that the choice of electrode material has a significant effect on the observed electrochemical signature in terms of the electrode's geometry, choice of composition and surface structure. Mass transport of the electroactive analyte under investigation is governed by the Nernst–Planck equation, as defined by:

$$J_i(x) = -D_i\frac{\partial C_i(x)}{\partial x} - \frac{z_i F}{RT}D_i C_i\frac{\partial \phi(x)}{\partial x} + C_i V(x) \qquad (5)$$

where $J_i(x)$ is the flux of the electroactive species $i$ (mol $s^{-1}$ $cm^{-2}$) at a distance $x$ from the electrode surface, $D_i$ is the diffusion coefficient ($cm^2$ $s^{-1}$), $\frac{\partial C_i(x)}{\partial x}$ is the concentration gradient at distance $x$, $\frac{\partial \phi(x)}{\partial x}$ is the potential gradient, $z_i$ and $C_i$ are the charge (dimensionless) and concentration (mol $cm^{-3}$) of species $i$ respectively and $V(x)$ is the velocity (cm $s^{-1}$) with which a volume element in solution moves along the axis.[40] These three key terms comprising eqn (5) represent the contributions to the flux of species $i$, that is, diffusion, migration and convection respectively. Note that flux is equal to current divided by $nFA$, where $n$ is the number of electrons transferred in the electrochemical process and $A$ is the electrode area ($cm^2$). If we consider voltammetry conducted in a solution which has supporting electrolyte and in stagnant solutions (non-hydrodynamic conditions) such that migration and convection can be neglected from eqn (5), this is thus reduced to consider the only relevant mode of mass transport to the electrode surface on the experimental time scale, which is diffusion. Let us consider a simple redox process involving the transfer of one-electron between the electrode and species A in solution to form the product B in solution, as shown below;

$$A + e^- \underset{k_a}{\overset{k_c}{\rightleftharpoons}} B \qquad (6)$$

where the rate of electron transfer is fast compared to the rate of mass transport, *i.e.* an electrochemically and chemically reversible redox process. Assuming that the electron transfer follows Butler–Volmer kinetics,

$$k_c = k_c^o \exp\left(\frac{-\alpha F}{RT}\eta\right) \qquad (7)$$

and

$$k_a = k_a^o \exp\left(\frac{\beta F}{RT}\eta\right) \qquad (8)$$

where $k^o$ is the standard electrochemical rate constant, $\alpha$ and $\beta$ are transfer coefficients such that $\alpha + \beta = 1$, and $\eta$ is the overpotential defined as:

$$\eta = E - E^{o'}_{A/B} \qquad (9)$$

where $E$ is the electrode potential and $E^{o'}_{A/B}$ the formal potential for the A/B couple. As the electrolysis of A progresses, all of the species A at the electrode surface will be consumed, resulting in a depletion of the concentration of A in the vicinity of the electrode surface and setting up a concentration gradient down which fresh A must diffuse from bulk solution to support further electrolysis. This depletion zone is known as the diffusion layer, the thickness of which, $\delta$, increases in size as a function of time, $t$, such that (in one-dimension):

$$\delta = \sqrt{2Dt} \qquad (10)$$

The diffusion of A from bulk solution to the electrode is described by Fick's first and second laws of diffusion;

$$j = -D\frac{\delta C}{\delta x} \qquad (11)$$

and

$$\frac{\delta C}{\delta t} = D\frac{\delta^2 C}{\delta x^2} \qquad (12)$$

where $j$ is the flux in mol $cm^2$ $s^{-1}$, $D$ the diffusion coefficient in $cm^2$ $s^{-1}$ and $C$ is the concentration of the electro-active species in mol $cm^{-3}$. The cyclic voltammetric response can be discovered by solving the transport equations (in three-dimensions, $x$, $y$ and $z$):[43]

$$\frac{\delta[A]}{\delta t} = D_A\nabla^2[A] \qquad (13)$$

and

$$\frac{\delta[B]}{\delta t} = D_B\nabla^2[B] \qquad (14)$$

and applying eqn (7)–(9) as boundary conditions where the equations:[43]

$$E = E_{start} + \nu t \quad 0 < t < \frac{E_{end} - E_{start}}{\nu} \qquad (15)$$

and

$$E = E_{end} - \nu\left[t - \frac{(E_{end} - E_{start})}{\nu}\right] \qquad (16)$$

define the potential sweep between $E_{start}$ and $E_{end}$ with a voltage sweep rate of, $\nu$, V $s^{-1}$ and $D_A$ and $D_B$ are the diffusion coefficients of A and B, respectively. Fig. 4 shows a typical cyclic voltammetric curve for the case of the electrochemical process as described in eqn (6) where a voltammetric potential is applied and the current monitored which gives rise to the unique profile presented in Fig. 4A. Note that characteristics of the voltammogram which are routinely monitored and reported are the peak height ($I_P$) and the potential at which the peak occurs ($E_P$).

Fig. 4A depicts the case for an electrochemically reversible process with fast electron transfer where it is evident that the peak-to-peak separation ($\Delta E_P = E_P^{ox} - E_P^{red}$) is relatively small. For the case of $n$ electrons, the peak-to-peak separation ($\Delta E_P$) depends on:

$$\Delta E_P = 2.218\frac{RT}{nF} \qquad (17)$$

Such that the peak currents are separated by a potential of 56.9 mV (*via* eqn (17) at 298 K where $n = 1$). Also shown in

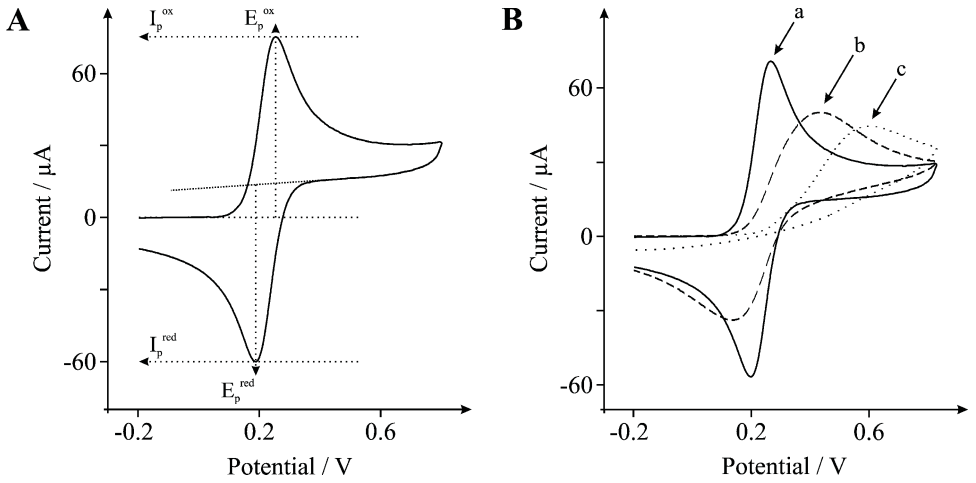


**Fig. 4** A: Typical cyclic voltammogram depicting the peak position $E_P$ and peak height $I_P$. B: Cyclic voltammograms for reversible (a), quasi-reversible (b) and irreversible (c) electron transfer.

Fig. 4B is the cyclic voltammetric response for an irreversible electrochemical couple (where the $\Delta E_P$ is larger than that observed for the reversible and quasi-reversible case) where appreciable over-potentials are required to drive the reaction, as evidenced by the peak height occurring at a greater potential than that seen for the reversible case.

In Fig. 4 it is evident that as the standard electrochemical rate constant, $k^o$, is either fast or slow, termed 'electrochemically reversible' or 'electrochemically irreversible' respectively, changes in the observed voltammetry are striking. It is important to note that these are relative terms and that they are in relation to the rate of mass transport to the electrode surface. The mass transport coefficient, $m_T$, is given by:

$$m_T = \sqrt{\frac{D}{(RT/F\nu)}} \tag{18}$$

The distinction between fast and slow electrode kinetics relates to the prevailing rate of mass transport given by '$k^o \gg m_T$' indicating electrochemical reversibility or '$k^o \ll m_T$' indicating electrochemical irreversibility. Matsuda and Ayabe[41] introduce the parameter, $\zeta$, given by:

$$\zeta = k^o/(FD\nu/RT)^{1/2} \tag{19}$$

where the following ranges are identified at a stationary macroelectrode: '$\zeta \geq 15$' corresponds to the reversible limit, '$15 > \zeta > 10^{-3}$' corresponds to the quasi-reversible limit and '$\zeta \leq 10^{-3}$' corresponds to the irreversible limit. Thus returning to Fig. 4, we have three cases, reversible, quasi-reversible and irreversible which are all related to the rate of mass transport. In reversible reactions the electron transfer rate is, at all potentials, greater than the rate of mass transport and the peak potential is independent of the applied voltammetric scan rate. In the case of quasi-reversible the rate of electron transfer becomes comparable to the mass transport rate. In this regime, the peak potentials increase with the applied scan rate. Last, it is obvious that for the irreversible case electron transfer rates are smaller than the rate of mass transport; the summary by Matsuda and Ayabe is extremely useful.[41] At macroelectrodes the Nicholson method is routinely used to estimate the observed standard heterogeneous electron transfer rate for quasi-reversible systems using the following equation:[42]

$$k^o = \psi\left[D_o\pi\left(\frac{nF\nu}{RT}\right)\right]^{1/2} \Big/ \left(\frac{D_o}{D_r}\right)^{\alpha/2} \tag{20}$$

where $\psi$ is the kinetic parameter and is tabulated at a set temperature for a one-step, one electron process as a function of the peak-to-peak separation ($\Delta E_P$) where one determines the variation of $\Delta E_P$ with $\nu$ and from this, the variation in the $\psi$. $D_o$ and $D_r$ are the diffusion coefficients of the oxidised and reduced species. For more accurate results in determining $k^o$, recourse to electrochemical simulation packages such as Digisim™ is advised.

The magnitude of the current observed at a macroelectrode is governed by the Randles–Ševćik equation for a fully reversible electron transfer process:

$$I_{P,Rev} = 0.446FAC(FD\nu/RT)^{0.5} \tag{21}$$

or alternatively for the case of a fully irreversible electron transfer process:

$$I_{P,Irrev} = 0.496(\alpha n')^{0.5}nFAC(FD\nu/RT)^{0.5} \tag{22}$$

where $A$ is the geometric area of the electrode ($cm^2$), $\alpha$ is the transfer coefficient (usually assumed to be close to 0.5), $n$ is the total number of electrons transferred in the electrochemical process and $n'$ is the number of electrons transferred before the rate determining step.

At a macroelectrode, electrolysis of A occurs across the entire electrode surface such that the diffusion of A to the electrode or B from the electrode surface is termed planar, and the current response is typically described as 'diffusion limited', giving rise to an asymmetric peak as shown in Fig. 5A. At the edge of the macroelectrode, where the electrode substrate meets the insulting material defining the electrode area, diffusion to or from the edge of the electrode is effectively to a point. Therefore, the flux, $j$, and the rate of mass transport are larger at the edge and as such diffusion becomes convergent. This is termed an 'edge effect' which is negligible at a macroelectrode since the contribution of convergent diffusion to the

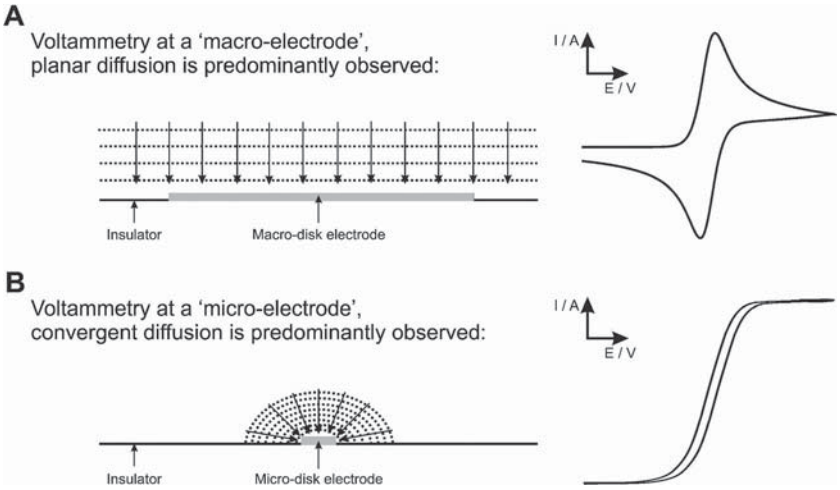


**Fig. 5** Highlighting the unique differences between the cyclic voltammetric signatures observed at a macroelectrode (A) compared to a microelectrode (B).

edges of the macroelectrode is inundated by that of planar diffusion to the entire electrode area.

As the electrode size is reduced from macro to micro, or even smaller to that of nano, convergent diffusion to the edges of the electrode becomes significant. In this regime a change in the observed voltammetric profile is observed which results in the loss of the peak shaped response, as evident in Fig. 5B with that of a sigmoidal voltammogram. The effect of convergent diffusion has the benefit of improvements in mass transport such that the current density is greater than at a macroelectrode under planar diffusion. Further information on electrochemistry and cyclic voltammetry can be sought from elegant books, see ref. 44 for examples. We next consider the electrochemical response at a HOPG electrode surface.

### 2.2. Electrochemistry of heterogeneous graphitic surfaces

Elegant work by Compton and co-workers[13] has allowed the electrochemical characteristics of HOPG to be fully understood and confirms that edge plane sites/defects are the predominant origin of electrochemical activity. Fig. 6A shows a schematic representation of the heterogeneous HOPG surface which has the two distinctive edge plane and basal plane sites, each with their own electrochemical activity and thus differing Butler–Volmer terms, $k^{o}$ and $\alpha$.

Using a simple redox couple, Fig. 7 depicts the voltammetry obtained when using either a Basal Plane Pyrolytic Graphite (BPPG) (i) or (ii) an EPPG electrode of HOPG, and the responses are compared with numerical simulations (iii) assuming linear diffusion only, in that, all parts of the electrode surface are uniformly (incorrectly) electrochemically active. Two features of Fig. 7 are evident: (1) there is a significant increase in the peak-to-peak separation, $\Delta E_P$, observed for (iii) over the EPPG voltammetric response (ii); (2) the fit to the 'linear diffusion' only (iii) simulation is not fully satisfactory, especially in the return scan where a significantly lower back peak (current) is observed than expected.[45] Interestingly, the exact voltammetric signature (i) can be correctly and quantitatively simulated through considering the HOPG surface (as shown in Fig. 1 and 6A) to be a heterogeneous surface consisting of edge

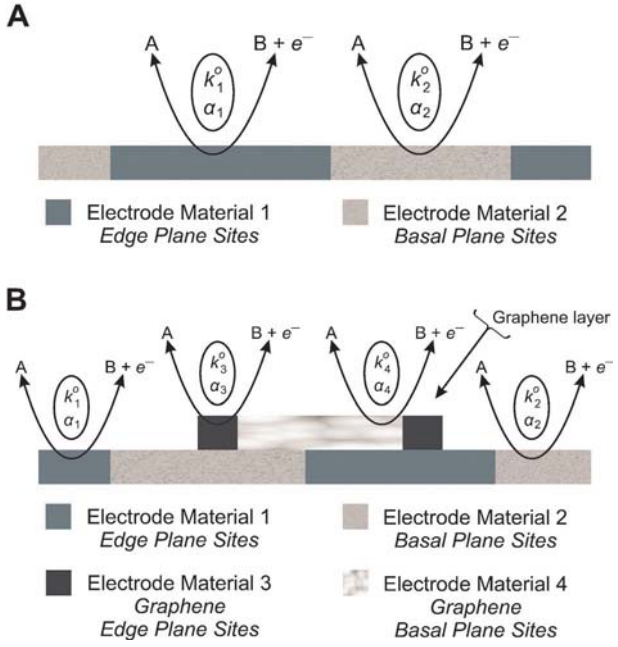


**Fig. 6** A: Schematic representation of an electrochemical reaction occurring on the same electrode surface with different Butler–Volmer characteristics. B: Following modification of surface A with graphene which has its own heterogeneous surface. Note that Fig. 6B is obviously not to scale.

plane nano bands which have been concluded to be exclusively the sites of electro-catalysis whereas the basal plane 'islands' are electro-catalytically inert.[13]

Fig. 8 depicts how the HOPG surface has been simulated using numerical simulation *via* the diffusion domain approach, where each basal plane island and the surrounding edge-plane band is considered as a circular disc of edge-plane graphite partially (or almost completely) covered with basal plane graphite, such that the areas of edge and basal plane are consistent. Since the island and band are surrounded by other island/band combinations, little or zero net flux of electroactive species will pass from one island to its neighbour.[13,45]

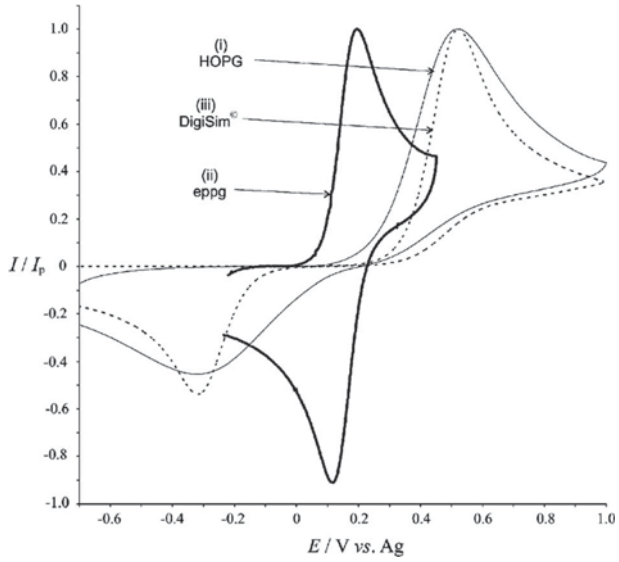


**Fig. 7** Cyclic voltammograms recorded at 1 V $s^{-1}$ for the oxidation of 1 mM ferrocyanide in 1 M KCl at a basal plane HOPG electrode and an EPPG electrode. The dashed line voltammogram is the simulated fit using linear diffusion only. Reproduced from ref. 45 with permission of The Royal Society of Chemistry.

The circular discs are treated as independent entities with cylindrical walls through which no net flux can pass. These unit cells are better known as diffusion domains and are illustrated in Fig. 8 where the two electrode materials are highlighted. The voltammetric response of the whole electrode is the sum of that for every domain on the electrode surface.

Fig. 8 illustrates a single diffusion domain unit cell and the cylindrical polar coordinate system employed where interacting cylindrical units of radius $R_0$ are centred around a circular block of radius $R_b$, where the fractional coverage of the domain, $\theta = R_b^2/R_0^2$ such that the surface areas of the basal sites and edge sites are given by $(1 - \theta)\pi R_0^2$ and $\theta\pi R_0^2$ respectively, which allows the effect of varying the edge sites while keeping the surface coverage constant. The island radius is termed as $R_b$ and $R_0$ is the domain radius which includes the width of the edge plane site/band. As is evident from Fig. 9, the $\Delta E_P$ of the edge plane nano band signal depends strongly on the edge plane coverage, and the domain size has little or no influence on the observed voltammetry of the three smaller domains due to the depleting effect of non-linear diffusion which becomes less relevant as the domain sizes increase. Note that the maximum lateral grain size of HOPG is 1–10 μm resulting in a maximum $R_0$ of ~0.5–5 μm, the edge plane coverage is such that the basal plane is effectively inert[45] and the HOPG response can be assigned to nano bands of edge plane graphite with the basal plane islands having no contribution.

More work from the Compton group has emerged exploring the double peak concept,[46] modelling a HOPG surface as an array of microbands; the unit cell is shown in Fig. 10A. Fig. 11 shows the response of an electrochemically heterogeneous surface highlighting the effect of microband width along with the domain coordinates utilised where the fractional coverage of the surface covered is given by: $\theta_{band} = r_{band}/r_{domain}$. Fig. 11A shows that as the width of the band is increased the diffusion profile changes from being largely convergent, as shown schematically in Fig. 10B, to that of linear which is seen as one peak becoming two and a decrease in the peak current is also evident. The depletion of the electroactive species above the electrochemically slower substrate proceeds to a greater extent so the substrate has less of an influence on the diffusion of the electroactive species and thus less of an influence on the observed voltammetry.[46] The depletion, known as the diffusion layer, is given by eqn (10) where for voltammetry $t$ can be replaced with: '$\Delta E/\nu$' where $\Delta E$ is the potential range over which electrolysis has occurred, thus $t$ (or $t_{peak}$: see below) is the time taken to sweep the potential from its initial value to the point where the current reaches a maxima. It has been shown that:[46]

$$\sqrt{2Dt_{peak}} \gg r_{sep} \text{ where } r_{sep} = \tfrac{1}{2}(r_{domain} - r_{band}) \qquad (23)$$

where $r_{band}$ is the width of the edge plane site and $r_{domain}$ accounts for the edge plane site *plus* the basal plane site (see Fig. 10A). In this case, the inter-band separation is small compared to the extent of diffusion parallel to the electrode surface and only one peak will be observed in the voltammetry. Fig. 11B shows the effect of the band width upon $k^o_{subs}$ and in which region split peaks will be observed. In the case that there is a large domain width, $\sqrt{2Dt_{peak}} \ll r_{sep}$, such that the voltammetry will be a superposition of the voltammetry of the band and substrate in isolation where diffusion to each will be linear in nature. If the heterogeneous rate constants on the two surfaces are similar, two peaks will be observed at similar potentials and will merge to form one larger peak. Note however, that if $k^o_{band} \gg k^o_{subs}$ (*i.e.* $k^o_{edge} \gg k^o_{basal}$) two peaks will be observed if the $k^o_{subs}$ has measurable activity; however it has been shown that this is not the case and only the $k^o_{band}$ is active, or sometimes reported as anomalously faster over that of $k^o_{subs}$.[12]

The rate of electron transfer for basal plane sites has been determined to correspond to $\sim 10^{-9}$ cm $s^{-1}$ for the oxidation of ferrocyanide and possibly even zero.[12–14] *How do we know that this is actually correct?* As shown in Fig. 9C, a strangely distorted voltammogram would be observed in the limit of very low defect density.[45] Due to the fact that two peaks have never been observed as shown from numerical simulations, it is generally accepted that edge plane electron transfer kinetics are anomalously faster over that of basal plane; this is sometimes referred to as being inert.[13,45] Interested readers are directed to the elegant work of Davies *et al.* and Ward *et al.* to further appreciate this work.[13,46] Last, other compelling data to define edge plane sites as the sites of electron transfer has been conducted by Davies *et al.*[12] by selectively blocking the basal plane sites of HOPG with a polymer whilst the edge plane sites were left exposed. Identical voltammetric behaviour was observed with this modified surface when compared to that of the initial bare/unmodified electrode and with numerical simulations, confirming the edge planes to be the sites of electrochemical activity.

### 2.3. Fundamental electrochemistry of graphene

When graphene is immobilised upon an electrode surface, as is common practice in the literature to electrically 'wire' graphene

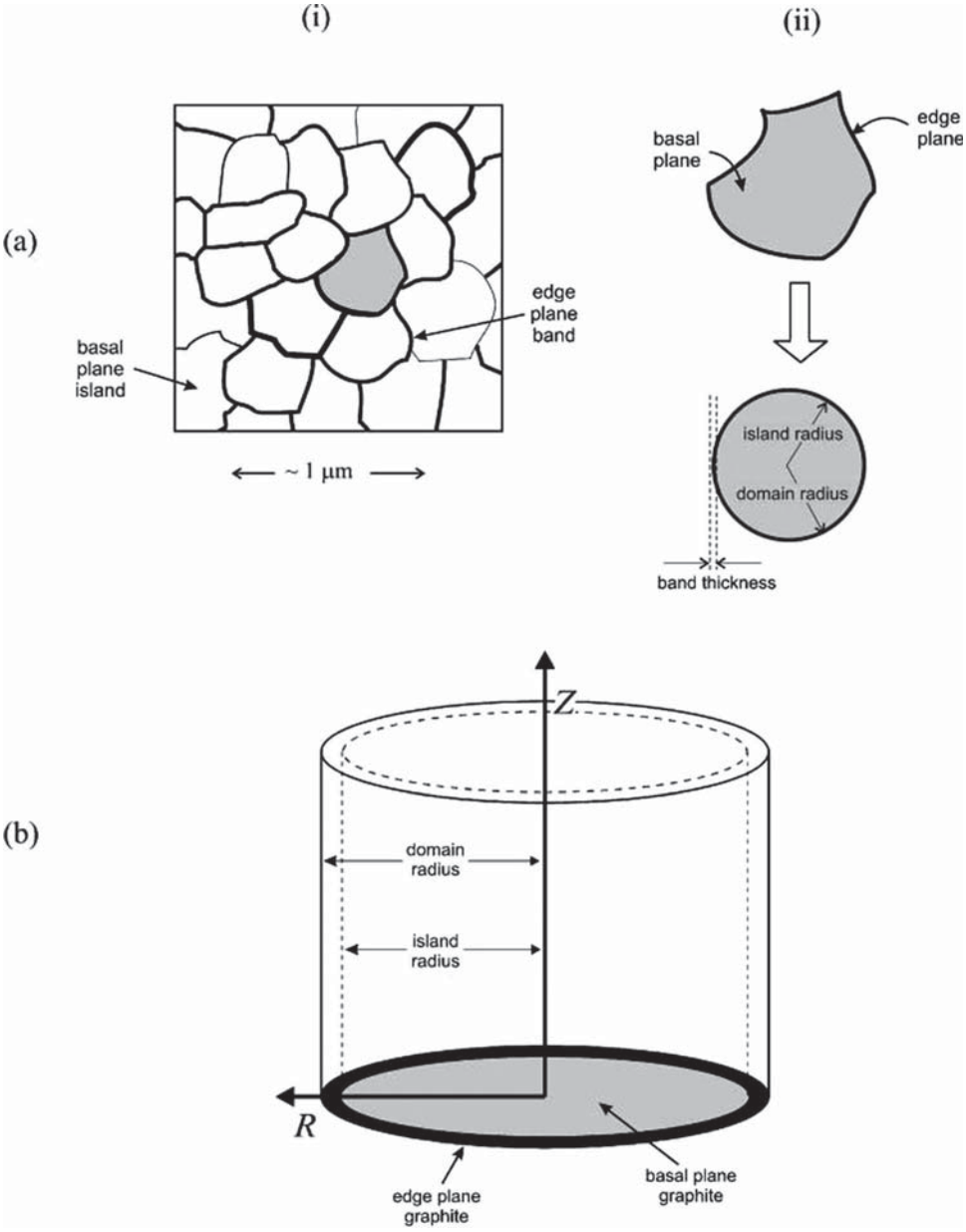


**Fig. 8** Schematic diagrams showing: (a), (i) the overhead view of a section of the basal plane HOPG surface and (ii) the approximation of each island/band combination as a partially covered circular disc of the same area; (b) the resulting diffusion domain from the approximation in (a) (ii) and the cylindrical coordinate system employed. Reproduced from ref. 45 with permission of The Royal Society of Chemistry. Note that the island radius is termed $R_b$ and the domain radius is $R_0$.

and study its electrochemical activity, a heterogeneous electrode surface is formed (note however that the number of contributing heterogeneous factors depends on the underlying surface utilised to support the said graphene). In this scenario (utilising HOPG, see above), the surface is represented by four key elements as shown in Fig. 6B. In addition to the underlying electrode surface (HOPG) which has edge plane and basal plane sites, each with the their own electrochemical activity with different Butler–Volmer terms, $k^o$ and $\alpha$ (see above), the introduction of graphene with its own edge and basal plane sites with their own $k^o$ and $\alpha$ values makes this an interesting situation. Note that in the case of modifying a metallic electrode as is sometimes spuriously undertaken, such as a gold macroelectrode, there would be three key electrochemical sites, the underlying gold ($k^o_{gold}$, $\alpha_{gold}$) and modified graphene with the contribution from edge and basal plane sites. However this is not a good situation as the underlying gold generally has (depending on the electroactive analyte) a greater electrochemical activity which dominates over the graphene (or other graphitic materials which could be employed) such that the contribution from graphene will not be observed or could be misinterpreted as graphene exhibiting excellent electrochemical activity if control experiments (bare/unmodified gold electrode) are not diligently undertaken.

Returning to the case of graphene (Fig. 6B) and utilising the insights discussed above from numerical simulations and

 

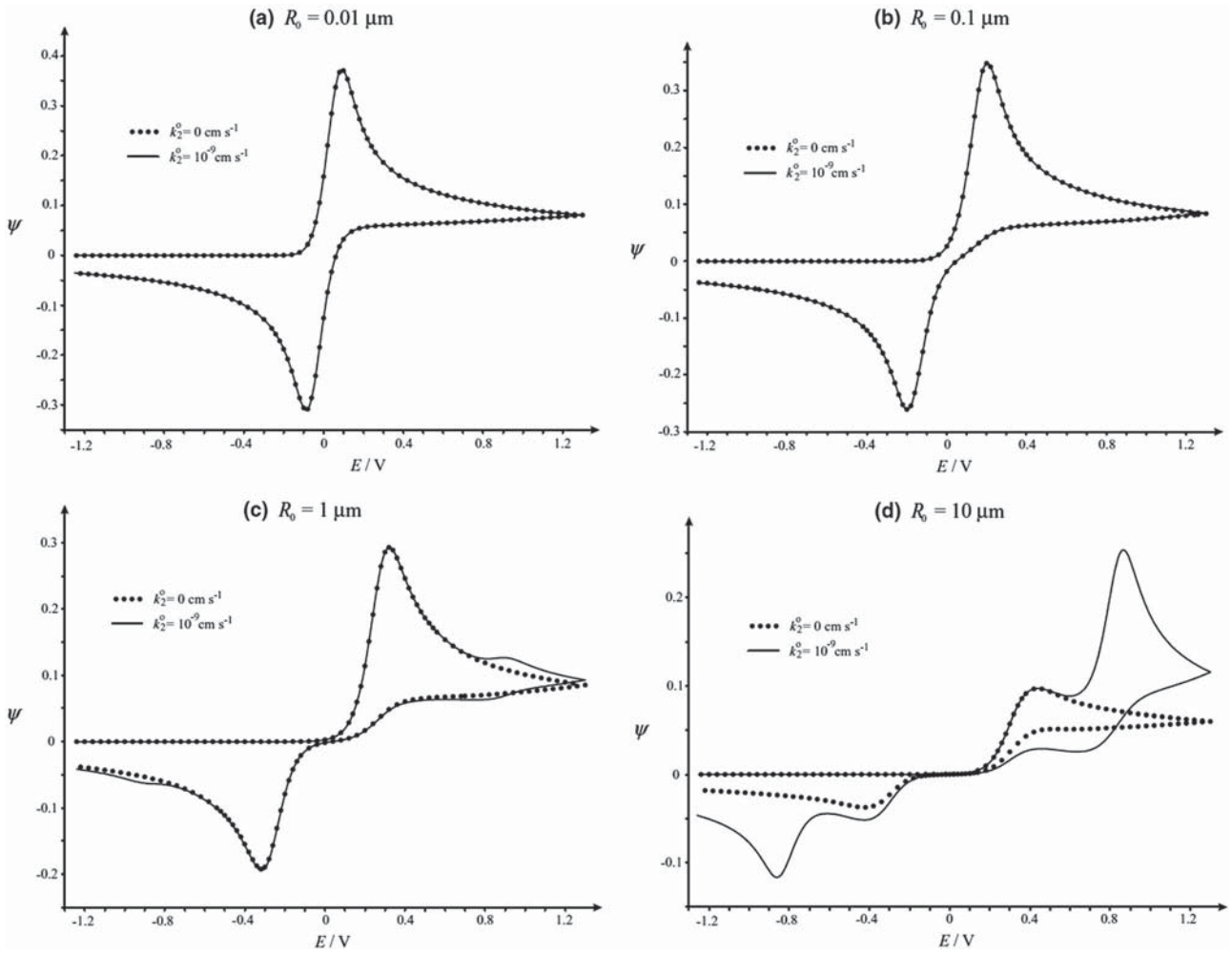


**Fig. 9** Solid curves are simulated dimensionless current cyclic voltammograms for diffusion domains where $D = 6.1 \times 10^{-6}$ cm$^2$ s$^{-1}$, $k_1^o = k_{edge}^o = 0.022$ cm s$^{-1}$, $k_2^o = k_{basal}^o = 10^{-9}$ cm s$^{-1}$, $\nu = 1$ V s$^{-1}$, the band thickness is 1.005 nm and the domain radius is (a) 0.01 μm, (b) 0.1 μm, (c) 1 μm and (d) 10 μm. Overlaid in each section are the simulated inert equivalents (dotted curves), *i.e.*, $k_2^o = k_{basal}^o = 0$ cm s$^{-1}$. Reprinted from ref. 13 with permission from Elsevier.

experimental observations for graphitic electrodes, *should graphene be considered similar to that of HOPG but as a single layer?*

In terms of graphene, the flake sizes of graphene that have been reported range from 75, 275 and 1500 nm in radius.[34] If we assume that graphene is immobilised upon an electrode surface laying parallel rather than vertical, we can approximate this graphene modified electrode surface to that shown in Fig. 8 where we have edge plane sites (*viz* the peripheral edge of graphene, and assuming no defects across the basal surface for simplification) and basal plane sites, the same unit cell approach *via* the diffusion domain method will be applicable in that we have islands with nano edge bands of thickness which, at best, might approximate to the length of a carbon–carbon bond which is reported to be ~0.142 nm in graphene. This can be assumed to be constant in many different forms of graphene with the expectation that the domain radius changes (*viz* the $L_a$ size) as the size of the graphene flake is either increased or decreased depending on its fabrication methodology. If we assume, in the first instance that the edge plane has fast electron transfer activity and that the basal plane has some negligible activity (~$10^{-9}$ cm s$^{-1}$), the effect of domain radius can be readily observed from inspection of Fig. 9, showing that at a large domain radius two peaks might be observed. However, to date such voltammetry has not been presented, adding weight to the inference that the edge plane side of graphene is the electroactive site acting akin to an edge plane nano band; this is a reoccurring theme which we explore later with experimental evidence from throughout the literature. Thus in the case of modifying a HOPG surface with graphene it is likely that the basal plane HOPG surface (BPPG), the $k_{basal}^o$ can be neglected such that Fig. 6B simplifies to two key domains, $k_{edge}^o$ (HOPG) and $k_{edge}^o$ (graphene), and assuming these are electrochemically similar in terms of the DOS, it is clear that edge plane sites are the key dominating factor of a graphene modified electrode.

**2.3.1. Graphene as a heterogeneous electrode surface.** Carbon based electrode materials have long been utilised within electrochemistry, they have out-performed the traditional noble metals in many significant areas and are at the forefront of innovation in this field.[11] This diverse and sustained success is due to carbons structural polymorphism, chemical stability, low cost, wide operable potential windows, relative inert electrochemistry,

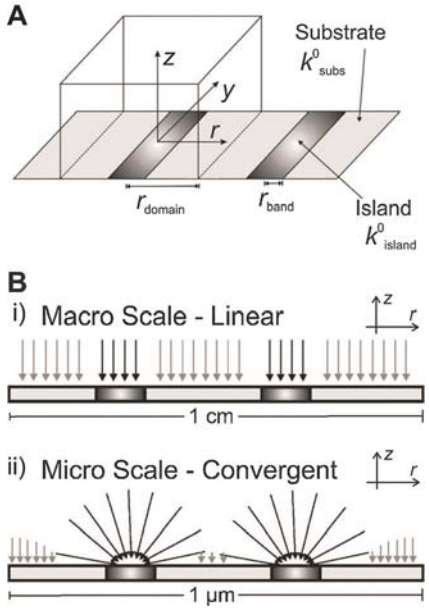


**Fig. 10** A: The surface is split into a series of identical domains (unit cells), namely band islands. B: Schematic difference between diffusion to macro- (i) and micro- (ii) scale electrode systems. The darker area represents the island ($r_{band}$) with the faster kinetics. Reproduced from ref. 46 with permission of The Royal Society of Chemistry.

rich surface chemistry and electro-catalytic activities for a variety of redox reactions.[9,11]

The electrochemistry of true graphene (*viz* an individual monolayer crystal) has been reported by Li *et al.*[47] where an ultra-microelectrode response was observed (steady-state current). The effective area of the graphene electrode was deduced from the planar disc ultra-microelectrode model as given in the following equation:

$$A_{\text{eff}} = \pi\left(\frac{i_{\text{ss}}}{4nFDC}\right)^2 \qquad (24)$$

where $A_{\text{eff}}$ is the effective area of an ultra-microelectrode and $i_{\text{ss}}$ is the steady-state current. From this equation the $A_{\text{eff}}$ of the graphene electrode was estimated to be 117 ± 8 $\mu m^2$, corresponding well with the geometric area that was measured independently *via* Atomic Force Microscopy (AFM), found to correspond to 130 $\mu m^2$.[47] The standard electrochemical rate constant was deduced for FcMeOH to be ~0.5 cm $s^{-1}$ indicating an electrode with fast electron transfer kinetics.[47] The authors' infer that improvements in the electron transfer kinetics (observed when contrasted to the basal plane of HOPG) are due to corrugations in the graphene sheet,[47] or could arise from edge plane like-sites/defects across the basal plane surface of the graphene in addition to exposed edges acting like ultra-microelectrodes with the sigmoidal voltammetry arising from the change in mass transport – the observations and inferences are highly fascinating, indicating why graphene is being fundamentally studied.

Recently the electrochemistry of individual single and double layered graphene crystals has been reported by Dryfe and co-workers.[48] Dryfe *et al.* performed time consuming experiments producing single mono-, bi- and multi-layer graphene crystals *viz* mechanical exfoliation ('scotch tape method') after which the authors electrically connected their graphene samples and encapsulated them with epoxy such that only the basal plane site (side) of graphene was exposed to the solution.[48] Sigmoidal currents were obtained using the potassium ferro-/ferri-cyanide redox probe due to the exposed graphene surface effectively being a large microelectrode.[48] Fig. 12 shows the current responses at a graphene mono-, bi- and multi-layer. Given that the edge of the graphene is covered with insulating epoxy and only its basal plane sites are exposed, it is surprising to observe any voltammetry at all. The reason for this observed voltammetry is that defects across the graphene surface reside,[48] where there is a missing lattice atom and as such a dangling bond is exposed providing electrochemical sites across the surface of the graphene,[49] most probably due to the mechanical stress involved in obtaining graphene from graphite using the 'scotch tape' (mechanical exfoliation) method. The sigmoidal response is due to the small size of the graphene sheet acting like a microelectrode (see Fig. 5). Note that defects across the basal surface of graphene are hard to determine and one approach is to use TEM and Scanning Tunnelling Microscopy (STM); Fig. 13 shows a typical defect observed in graphene with TEM, Density Functional Theory (DFT) simulation of a graphene defect and an experimentally observed defect *via* STM.[49] Note also that the effect of defects on HOPG is well known in that a 1% defect density is estimated to result in a $10^3$ factor increase in the heterogeneous electron transfer rate constant.[50] Dryfe *et al.* demonstrate that while their graphene surface has a low level of defects, fast electron transfer is observed due to the defects that are present on the graphene surface[48] and resultantly a similar voltammetric response is observed at bi-layer graphene (see Fig. 12) due to the top graphene layer only being exposed. Such work indicates that surface defects are extremely important in obtaining fast electron transfer, which has been shown for pristine graphene (see later).[51]

Note that the above reports are currently the only two examples in the literature where individual graphene crystals have been electrochemically probed and the reason as to why this is, is due to the large amount of effort that one has to undertake in order to perform such experiments. Clearly these are fundamental studies with the fabrication not scalable such that the most common approach to utilise graphene is to immobilise it upon a suitable electrode surface such that one is effectively averaging a response over that of the graphene domains.

Using an approach as noted above, key insights into the electrochemical reactivity of pristine graphene have been provided recently by Brownson *et al.*[51] who considered the modification of edge and basal plane pyrolytic graphite (EPPG and BPPG respectively) with pristine graphene, as is common place in the literature in order to 'electrically wire' the graphene. The authors utilised a plethora of electroactive probes that have been commonly employed within the field, are well characterised on graphitic materials and have been well understood over many decades. Surprisingly, such work was the first to show a deviation from the current wealth of literature on graphene. Pristine graphene was shown not to be as beneficial as previously reported. Due to the type of graphene utilised,

 

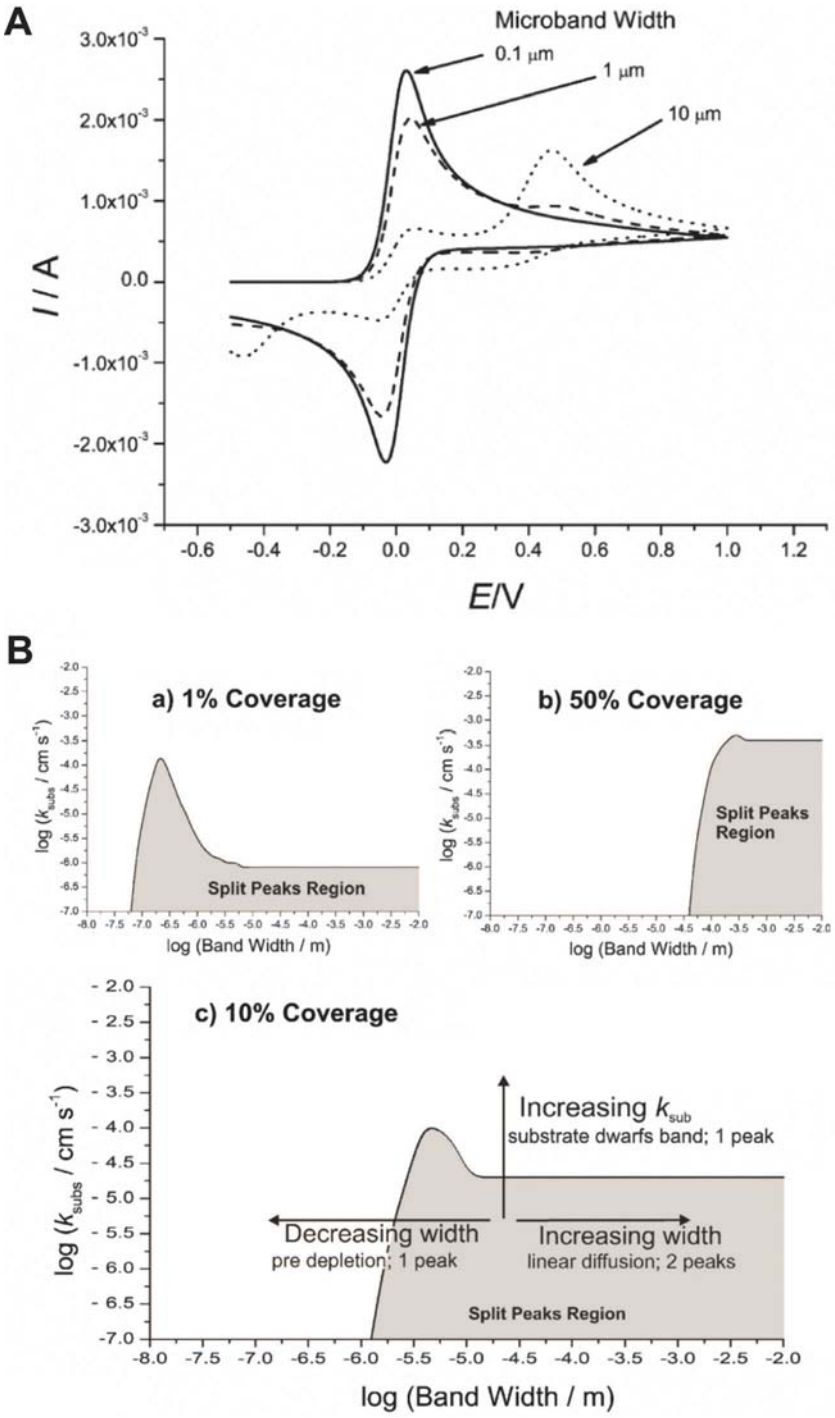


**Fig. 11** A: Voltammetry of a one-electron transfer process at an electrochemically heterogeneous electrode consisting of an array of microbands ($k^o = 10$ cm s$^{-1}$) distributed over a substrate material ($k^o = 10^{-6}$ cm s$^{-1}$) of area 1 mm$^2$ and a surface coverage of the bands of 10% at a scan rate of 0.1 V s$^{-1}$. The diffusion coefficient of all species is $10^{-5}$ cm$^2$ s$^{-1}$ with an initial concentration of 10 mM. The voltammetry transitions from 1 peak to 2 peaks as the width of the band (labelled) is increased. B: Schematics showing the region of the 'Band Width'-'Substrate rate constant' space for which there are two peaks in the forward sweep of a cyclic voltammogram at band surface coverages of (a) 1%, (b) 50% and (c) 10%. Scan rate = 0.1 V s$^{-1}$; diffusion coefficient = $10^{-5}$ cm$^2$ s$^{-1}$; island rate constant $k^o_{band} = 10$ cm s$^{-1}$. Reproduced from ref. 46 with permission of The Royal Society of Chemistry.

that is, high quality graphene with a low density of defects across the basal plane surface of the graphene sheet as well as a low oxygen content, the authors observed that graphene exhibits slow electron transfer kinetics and the electrochemical response was found to actually block the underlying electrode surface.[51] Such a response is represented in Fig. 14 for the electrochemical oxidation of ferrocyanide. Shown in Fig. 14A is the response of a BPPG electrode following modification with graphite.

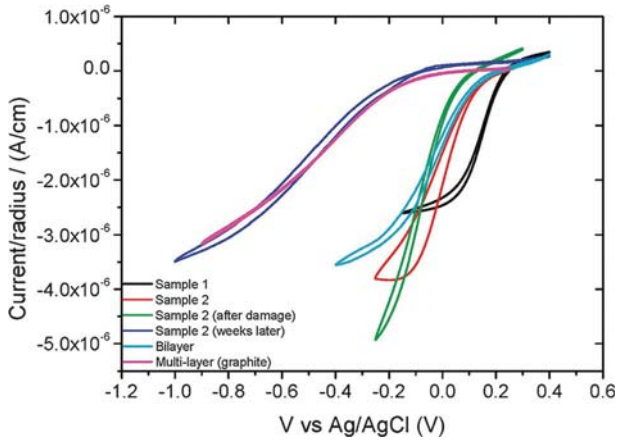


**Fig. 12** Ferricyanide voltammetry: Current (normalised to electrode radius) *vs*. potential response for the graphene monolayer samples (Samples 1 and 2: 1, monolayer contained no visible defects and its edges were completely masked – note however that although special attention was paid during the masking and preparation of samples in order to expose areas with the minimum number of defects, the authors acknowledge that to date it has not been possible to achieve a perfect, edge-free region; 2, monolayer contains several holes of $\sim$10 μm diameter, hence some edge sites must be in contact with the electrolyte), a bilayer sample and the multilayer sample. Scan rate = 5 mV $s^{-1}$; concentration = 1 mM ferricyanide in 1 M KCl. Reprinted with permission from ref. 48. Copyright 2011 American Chemical Society.

It is well known that graphite has a large proportion of edge plane like-sites/defects and hence when one immobilises graphite, the underlying electrode surface which exhibited slow electron transfer (note the large $\Delta E_P$) exhibits a change (improvement) in the voltammetric signature due to the surface becoming populated with edge plane sites. In the case of graphene however (Fig. 14B), the reverse is observed, that is the introduction of graphene appears to be blocking the underlying electrode surface. In this case, when graphene was introduced onto a surface that exhibited fast electron transfer rates and a high degree of edge plane sites, the immobilised graphene blocked the underlying surface, reducing the overall electrochemical activity, which can be attributed *via* the fundamental knowledge on graphite electrodes to be due to the high proportion of relatively inert basal plane surface on pristine graphene as opposed to a small structural contribution from edge plane sites/defects.[51]

In terms of the coverage of graphene over a supporting substrate, it was indicated that two working zones were evident.[51] '*Zone I*' corresponds to the modification of the electrode surface which results in single- and few-layer graphene modified electrodes, which block the electrochemical response observed at the underlying electrode. Upon increasing amounts of graphene, the underlying electrode is continuing to be blocked (as shown in Fig. 14B). This is since the material (graphene) that is being immobilised has a low proportion of edge plane sites since the proportion of edge plane sites to basal plane sites (within its geometric structure) are extremely low and given its pristine nature, edge plane sites/defects across the basal surface are negligible.

Upon the addition of more graphene, a '*Zone II*' becomes evident.[51] This is where several/significant layers of graphene are observed (*viz* graphite) which leads to an increment in density of edge plane sites (due to its geometric structure) and thus improved voltammetry *via* increased heterogeneous electron transfer rates (as is evident in Fig. 14A). This response continues until a limit is observed, typically from the instability of the graphene upon the underlying electrode surface/support. Clearly the coverage of graphene is a key parameter in graphene electrochemistry, where the incorrect use/characterisation of a graphene modified surface could mislead those that are actually observing graphite (but believe they are using graphene) into misreporting the benefits of graphene, *i.e*. if working in *Zone II*.

Fig. 15 highlights the change in the structure of the electrode surface from introducing graphene and the resultant electrochemical responses expected. Fig. 15A shows a cyclic voltammetric profile as typically observed at an edge plane HOPG electrode assumed to possess fast electron transfer kinetics and following the immobilisation of single-layer graphene (Fig. 15B) an incomplete coverage is realised. Effectively one is replacing a highly efficient and reactive surface with graphene which has a low proportion of edge plane sites and no defects across the basal plane surface of the graphene, giving rise to the observed voltammetry with an increase in $\Delta E_P$ indicating a departure towards slower electron transfer kinetics.[51] Following complete single-layer coverage (Fig. 15C) of graphene the $\Delta E_P$ increases which is firmly in *Zone I* as identified above. As more graphene is immobilised (Fig. 15D), a departure from single-layer, or approximate single layer/double and few layer is evident to that of multi-layer graphene (*viz* graphite) where one is now in *Zone II*, such that the voltammetric response

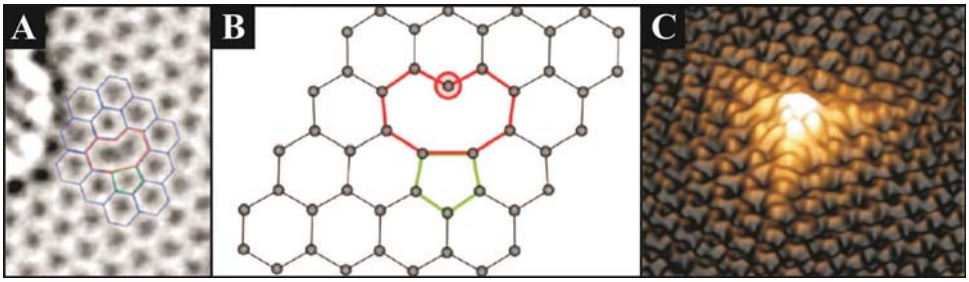


**Fig. 13** A: TEM image of a defect in a graphene lattice (Reprinted with permission from ref. 119. Copyright 2008 American Chemical Society); B: Simulated atomic structure obtained *via* DFT calculations (Reprinted with permission from ref. 49. Copyright 2010 American Chemical Society); C: An experimental STM image of a single vacancy, appearing as a protrusion due to an increase in the local DOS at the dangling bond (marked with a circle in panel B) (Reprinted with permission from ref. 120. Copyright 2010 The American Physical Society).

 

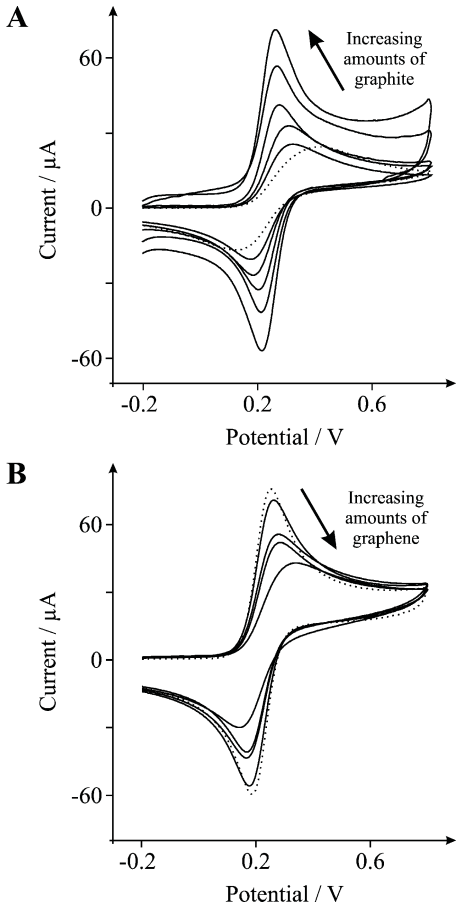


**Fig. 14** Cyclic voltammetric profiles recorded utilising 1 mM potassium ferrocyanide(II) in 1 M KCl. A: obtained using a BPPG electrode (dotted line) with the addition of increasing amounts of 2, 4, 50, 100, and 200 µg graphite (solid lines). B: obtained using an EPPG electrode (dotted line) with the addition of increasing amounts of 10, 20, 30, and 40 ng graphene (solid lines). Scan rate: 100 mV $s^{-1}$ (*vs.* Saturated Calomel Reference Electrode, SCE). Reproduced from ref. 51 with permission of The Royal Society of Chemistry.

heads back towards that originally observed for HOPG (Fig. 15A) due to the now large proportion of edge plane sites upon the electrode surface.[51]

Thus, Brownson *et al.* has shown that given the geometric structure of graphite (multiple layers of stacked graphene), by its very nature it possesses a larger proportion of edge plane sites than that of single layer graphene and thus the former exhibits improved electrochemical activity, heterogeneous electron transfer kinetics, over that of the latter.[51] In support of this work it has been shown recently, using SECM to study correlations in monolayer and multilayer graphene electrodes grown *via* CVD, that in terms of these layered structures, single layer graphene exhibits the lowest electrochemical activity and that the activity increases systematically with the number of layers, to a situation where the flakes are so active that the electron transfer process becomes nearly electrochemically reversible at greater than 7 layers (*viz* graphite).[53]

Returning to the case of immobilising pristine graphene onto a HOPG surface for electrochemical investigation (see above), insights from Brownson *et al.*[51] reveal that the underlying (supporting) electrode surface plays an important role, as does the orientation of the immobilised graphene. SEM images revealed that coalesced graphene 'folds' over edge plane sites of the underlying electrode, potentially explaining the blocking effect observed when graphene is introduced. Upon further additions of graphene, orientation with the edge plane sites of the underlying electrode results in a vertically aligned or disorder graphene surface and hence a beneficial increase in the electrochemical response is observed due to the increment in the proportion of edge plane sites accessible for electron transfer.[51] In this model it is assumed that the immobilised graphene adopts a similar architecture to that of the underlying electrode since the graphene has a distributed electron density of the planar–basal site (π–π) which will be disturbed by the high electron density of the underlying edge sites of the graphene (the EPPG) such that it effectively 'aligns' with the underlying electrode surface as this arrangement reflects the lowest energy settlement.[51] Due to the high number of graphene sheets on the EPPG the graphene sheets will stack (as a continuation of the edge planes) in parallel to each other in order to fit the limited space of the EPPG surface. In the case of graphene upon a BPPG electrode surface the graphene will follow the same architecture as presented by the BPPG sheets, meaning that the graphene will stack planar on the BPPG due to π–π stacking.

Last, insights from DFT simulations on different sizes of graphene reveal a greater electron density at the edge of pristine graphene which confirms the observations by Brownson *et al.*[51] and in other work[43,54] such that, similar to that observed for HOPG, the peripheral edge of graphene as opposed to its side acts electrochemically akin to that of edge plane sites and the latter to that of basal plane sites; in this case pristine graphene assumes no defects (defect sites, missing atoms, dangling bonds *etc.*) across the surface of the graphene, the introduction of which will beneficially contribute to the electrochemical activity of graphene. Note that in the case of graphite a greater density of edge plane sites is well known to result in an improved electrochemical reactivity,[11–14] but until recently this was lesser reported for graphene.

As such Lim *et al.*[55] have recently investigated the effect of edge plane defects on the heterogeneous charge transfer kinetics and capacitive noise at the basal plane of CVD fabricated epitaxial graphene (prepared on a silicon carbide substrate) using inner-sphere and outer-sphere redox mediators. The authors showed that the basal plane surface of graphene exhibits slow heterogeneous electron transfer kinetics, interestingly however, when electrochemically anodised (increasing the degree of oxygen-related edge plane defects) they found that the defects created on its surface result in the observation of superior election transfer rates that surpass those observed for pristine graphene, Glassy Carbon (GC) and Boron Doped Diamond (BDD) electrodes.[55] Such a response clearly highlights the essential need for edge plane like-sites/defects on the surface of graphene (for improved electrochemical reactivity). Note, it is well known that the presence of oxygen related species on a carbon based electrode material can dramatically influence the observed electrochemical reactivity (either beneficially or detrimentally depending on the target analyte).[9,56] As such it could be inferred that the oxygen-related species

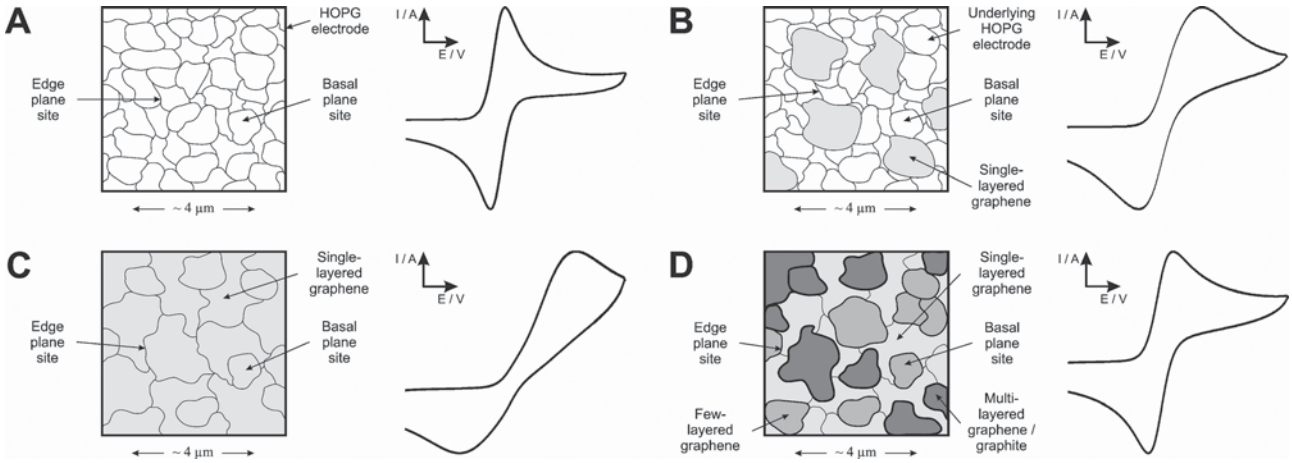


**Fig. 15** Schematic representation of the effect on the cyclic voltammetric profiles that will be observed for a HOPG electrode following modification with differing coverages of graphene using a simple outer-sphere electron transfer redox probe. (A) represents an unmodified HOPG electrode surface where fast electron transfer kinetics are observable, (B) after modification with graphene leading to incomplete coverage where reduced electron transfer rates occur, (C) after modification with graphene leading to complete single layer coverage where due to the large basal content of graphene (in contrast to edge plane) poor electrochemical activity is observed where electron transfer is effectively blocked, and (D) after continual modification with graphene leading to layered structures with increased edge plane sites available (origin of fast electron transfer) and thus an improvement in the electrochemical response is observed. Reproduced from ref. 51 with permission of The Royal Society of Chemistry.

## Box 1: Surface sensitivity at inner- and outer-sphere redox probes

It is important to note that a common approach within electrochemistry, in order to greater understand the material under investigation, is to utilise inner-sphere and outer-sphere redox mediators/probes. Thus it is wise to distinguish between an ''outer-sphere'' and an ''inner-sphere'' electron transfer process, which differ most significantly according to the 'sensitivity' of their electron transfer kinetics to the surface chemistry of the carbon electrode under investigation in terms of the surface structure/cleanliness (defects, impurities or adsorption sites) and the absence/presence of specific oxygen containing functionalities, that is, variations in $k^o$ with the condition of the electrode surface.[11,52]

Outer-sphere redox mediators (such as $Ru(NH_3)_6Cl_3$ and $K_2IrCl_6$) are termed *surface insensitive* in that the $k^o$ is not influenced by the surface oxygen–carbon ratio, surface state/cleanliness in terms of a surface coating of a monolayer film of uncharged adsorbates, or specific adsorption to surface groups/sites. Here there is no chemical interaction or catalytic mechanism involving interaction (*i.e.* an adsorption step) with the surface or a surface group – such systems often have low reorganisation energies;[11,52] in this case the electrode merely serves as a source (or sink) of electrons and as such outer-sphere systems are sensitive primarily to the electronic structure due to the electronic DOS of the electrode material.[11,52]

Conversely, inner-sphere redox mediators (such as $K_4Fe(CN)_6$ and $VCl_3$) are termed *surface sensitive* in that the $k^o$ is strongly influenced by the state of the electrode surface (surface chemistry and microstructure) *via* specific electro-catalytic interactions that are inhibited significantly if the surface is obscured by adsorbates (or impurities). Such interactions can also depend strongly on the presence (or absence) of specific oxygenated species which give rise to either beneficial or detrimental effects.[11,52] In this case systems are more largely affected by surface state/structure and/or require a specific surface interaction, being catalysed (or inhibited) by specific interactions with surface functional groups (adsorption sites) rather than the DOS as such systems generally have high reorganisation energies.[11,52]

Thus it is clear that the observation of differing responses when using varied inner- and outer-sphere redox probes allows insight to be deduced regarding the state of the surface structure of the electrode material in question. For more information interested readers are directed to the authoritative work of McCreery.[11,52]

purposely introduced onto the graphene surface in this case contribute to a hidden origin of the improved rate kinetics. However, this is not the case and the contribution from the oxygenated species residing on the graphene can be neglected since the authors utilised a range of electro-active species to study their graphene (from simple outer-sphere electron transfer probes to surface sensitive inner-sphere species, see Box 1) and the observed trend was similar for all compounds.

In further notable work that supports the above findings (that is, the edge plane of graphene is dominantly active over that of its basal plane) Keeley *et al.*[57] sonicated graphite powder in dimethylformamide for 72 hours to achieve exfoliation of graphene nanosheets, without the need for chemical oxidation – thus cleverly the authors alleviated any unnecessary contributions from the presence of surface oxygenated species. TEM analysis showed that 90% of the nanosheets contained five or fewer graphene layers and the lateral dimensions were mostly less than 1 mm, leading to a much higher density of edge plane-like sites than the parent graphite, as was confirmed by Raman spectroscopy. Cyclic voltammetric measurements with

 

common redox probes confirmed that nanosheet-functionalised electrodes had larger active areas and exhibited far more rapid electron transfer than the plain electrodes. Given the virtual absence of oxygen-containing groups in the solvent-exfoliated graphene, the researchers took this activity to originate from the numerous edge plane-like sites and defects on the nanosheets.[57] Moreover, further diligent work has been reported by the Pumera group who studied the influence of open and folded graphene edges on its electrochemical properties.[58] Pumera *et al*. found that the heterogeneous electron transfer rate is significantly lower on folded graphene edges (structurally more similar to basal plane sites) when compared to open edge sites for the ferro-/ferri-cyanide redox probe; as is evident in Fig. 16 where a larger $\Delta E_P$ is observed with regards to the former over that of the latter. Their work also demonstrated that the electrochemical properties of open edges were favourable over folded ones with regards to the lower over-potential detection of biomarkers.[58] It is apparent therefore, that for sensing and bio-sensing applications, folded edges are less active than open edges, which can thus be extended to concur with the concept concerning the coverage of edge plane sites as stated by Brownson *et al*. and thus higher edge plane content should then be preferred for such applications.[51]

On a final note, interesting work by Tan and co-workers[59] utilising SECM to study the reactivity of surface imperfections present on monolayer graphene supports the vital insights gained above regarding the reactivity of edge plane defects. Their work revealed that specific sites across the surface of monolayer graphene that have a large concentration of defects (introduced either through deliberate mechanical damage or through chemical oxidation) are approximately 1 order of magnitude more reactive, compared to more pristine graphene surfaces, toward electrochemical reactions.[59] Of further importance, the authors were able to successfully passivate the activity of graphene defects by carefully controlling the electropolymerisation of *o*-phenylenediamine so that a thin film of the polymer was formed (which was found to be insulating in nature toward heterogeneous electron transfer processes): thus it was demonstrated that SECM can be utilised for detecting the presence of (and ''healing'') surface defects on graphene; providing a strategy for *in situ* characterisation and control of this fascinating material and enabling optimisation of its properties for select applications.[59]

It is clear that there is a need to have exposed edges of graphene to achieve optimal electrochemical activity (fast electron transfer rates), or equivalently to have a high density of edge plane like-sites/defects across the graphene surface. As highlighted in Section 1.1 different preparative methods of graphene result in structures that have greatly varied densities of edge plane defects[34] and thus it has been shown that the method of graphene preparation consequently has a dramatic influence on the materials properties and electrochemical reactivity.[34,60] Furthermore, surface defects can be selectively introduced into the graphene structure post-synthesis *via* other means, for example through ion or electron irradiation, selective oxidation (with optional reduction), or by mechanical damage;[49] note that incorporation of dopants/foreign atoms (*i.e*. nitrogen doping) or the introduction of functionalities (*i.e*. oxygenated species) in addition to the formation of composite graphene based materials have also all been shown to alter the electrochemical properties of graphene either beneficially or detrimentally (in terms of the observed heterogeneous electron transfer rates, DOS, intrinsic catalytic attributes and influences on surface adsorption/desorption processes).[21,56,61] Importantly, if controllable and reproducible defect densities of graphene can be achieved (as has been shown to be the case at CVD graphene)[34] and efficiently quantified (see Section 2.3.4), it is evident that through varying such attributes the electrochemical reactivity of graphene can be optimised and efficiently tailored when designing graphene based devices with dedicated properties to achieve new functions/applications (to exhibit either fast or slow heterogeneous electron transfer – or to possess specific

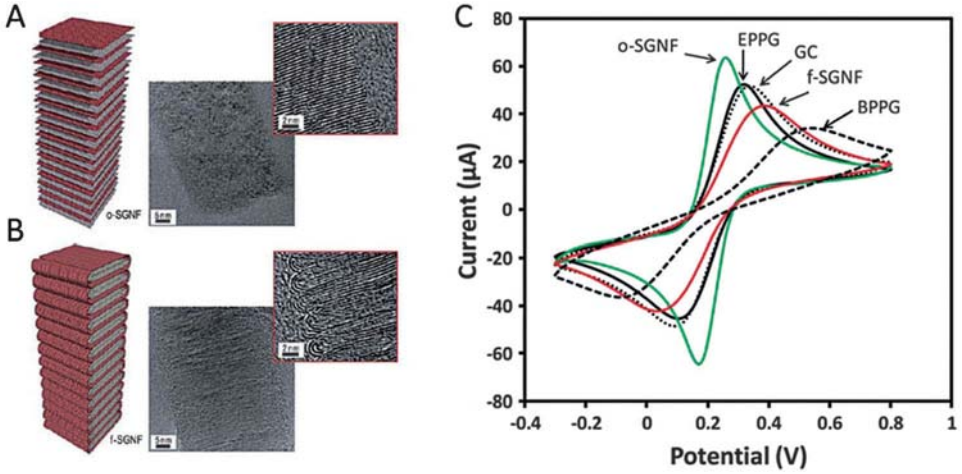


**Fig. 16** Electrochemistry at folded edges of graphene sheets. Schematic drawing and TEM micrographs of (A) open and (B) folded graphene edge nanostructures. The drawing is not to scale and it should be noted that the ''opening'' of the folded edge nanostructure is to illustrate the inner structure of the fibre. The structural difference between open (A) and folded (B) edges are clearly visible in the detailed images on the right. (C) Cyclic voltammograms of 5 mM potassium ferrocyanide(II) in 0.1 M KCl supporting electrolyte on open graphene structure (green; o-SGNF), folded graphene structure (red; f-SGNF), EPPG (solid line), GC (dotted line) and BPPG (dashed line) electrodes. Scan rate 100 mV $s^{-1}$ (*vs*. Ag/AgCl reference electrode). Reproduced from ref. 58 with permission of The Royal Society of Chemistry.

binding/attachment sites in the case of functionalisation). Thus effectively graphene provides a beneficial platform where it is possible to modify the graphene structure so that the properties of this material suit specific needs; such tailoring and versatility of is of eminent importance for practical applications as well as for academic research.

**2.3.2. Effect of surfactants on the electrochemistry of graphene.** As highlighted in Section 1.1 suspensions of graphene in a liquid are often (but not always) stabilised by surfactants, which are routinely incorporated into the fabrication of commercially available graphene to reduce the likelihood of the graphene sheets coalescing. Note that when this is the case a tentative approach must be employed when utilising such graphene solutions within electrochemistry.[62] It has been established that some surfactants, for example sodium cholate, exhibit measurable electrochemical activity and can thus contribute towards or even dominate the electrochemical properties and performance of the stabilised graphene, such that highly negative effects on the interpretation of data have been observed.[62] This was demonstrated to be the case towards the detection of β-nicotinamide adenine dinucleotide (NADH) and acetaminophen (APAP; paracetamol) as well as in the stripping voltammetry of heavy metals.[62a,b] These interferences/effects also extended to energy storage applications where it was demonstrated that surfactants themselves provide a higher capacitance than graphene, thus one must be cautious when attributing beneficial effects to graphene in these instances.[62d]

This work poses a highly important warning to the graphene community to always consider the effect/influence of any surfactant/solvent that is used to aid graphene dispersion. It is clear that appropriate control experiments need to be employed before the beneficial electrochemistry of graphene can be correctly reported and such control measures are thus required in future experiments in order to sufficiently de-convolute the true performance of graphene. Such a warning can be extended to other aspects of graphene electrochemistry, including the requirement for appropriate control and comparison experiments when determining the contribution to the electrochemical response of graphene in terms of the presence of graphitic impurities and oxygenated species (see later, Section 3).

**2.3.3. Metallic impurities on the electrochemistry of graphene.** When CNTs first exploded onto the scientific scene it was soon realised that metallic impurities, as a result of their fabrication process, contributed to the observed electrochemical response.[38] In a similar fashion, it has been shown that graphene fabricated from graphite (*via* chemical oxidation of natural graphite followed with thermal exfoliation/reduction) contains cobalt, copper, iron, molybdenum and nickel oxide particles which can influence the electrochemistry of graphene towards specific analytes, and has potential to lead to inaccurate claims of the electro-catalytic effect of graphene.[63] Note that while thorough physical characterisation of the graphite and fabricated graphene is clearly missing from this work,[63] it nicely highlights the importance of metallic impurities and it is clear that a pure source of graphite (or as higher purity that can be obtained) should be used in order to alleviate such problems; or purchase commercially available pure graphene from reputable suppliers. Nonetheless, as with Sections 2.3.2 and 2.3.7 this valuable work highlights the importance of sufficient control experimentation when exploring graphene within electrochemistry.

**2.3.4. Quantifying the electron transfer sites of graphene.** When performing experiments with graphene, there is a need to determine the proportion of electrochemical reactive sites such that experimentalists can recreate reported experiments. In the case of graphene and HOPG electrodes the electron transfer rate is usually referred to as the observed electron transfer rate, $k^{o}_{obs}$, due to the electrochemical response arising from the two structural contributions, edge plane and basal plane sites, which thus constitute a heterogeneous electrode surface with the overall electron transfer rate ($k^{o}_{obs}$) a function of these two contributions, $k^{o}_{edge}$ and $k^{o}_{basal}$ (see Fig. 1):

$$k^{o}_{obs}(\text{HOPG}) = k^{o}_{edge}(\theta_{edge}) + k^{o}_{basal}(1 - \theta_{edge}) \quad (25)$$

It has been elegantly shown that the electron transfer rate of the edge plane is much faster (infinitely faster) over that of the basal plane, which in comparison is relatively inert,[12] (see above) which allows us to write:

$$k^{o}_{edge} \gg k^{o}_{basal} \quad (26)$$

which leads eqn (25) to reduce to:

$$k^{o}_{obs}(\text{HOPG}) = k^{o}_{edge}(\theta_{edge}) \quad (27)$$

where the global coverage of edge plane defects ($\Theta_{edge}$) is approximate to the coverage of the edge plane ($\theta_{edge}$);[12]

$$\theta_{edge}(\text{HOPG}) \approx \Theta_{edge}(\text{HOPG}) \quad (28)$$

In the case of graphene, the edge plane of graphene is the origin of the observed electrochemical response,[51,54] allowing us to write for the case of graphene:

$$k^{o}_{obs}(\text{graphene}) = k^{o}_{edge}(\theta_{edge}) + k^{o}_{basal}(1 - \theta_{edge}) \quad (29)$$

which using the argument earlier allows us to write:

$$k^{o}_{obs}(\text{graphene}) = k^{o}_{edge}(\theta_{edge}) \quad (30)$$

where the global coverage is given by:

$$\theta_{edge}(\text{graphene}) \approx \Theta_{edge}(\text{graphene}) \quad (31)$$

Thus from the electrochemical response, which is due to electron transfer residing at the edge of graphene (graphitic materials), *viz* edge plane sites, for graphene immobilised onto an electrode surface, the global coverage of electron transfer sites can be readily determined from:

$$\frac{k^{o}_{obs}}{k^{o}_{edge}} = \Theta_{edge}(\text{graphene}) \quad (32)$$

as long as $k^{o}_{edge}$ has been rigorously determined. Assuming that graphene is structurally similar to that of HOPG islands when immobilised upon an electrode surface and that the electron transfer is due to the edge plane like-sites/defects. For the case of $[Ru(NH_3)_6]Cl_3$; $k^{o}_{edge} = 0.4$ cm $s^{-1}$.[12,13]

Using the earlier approach with eqn (32), the global coverage of edge plane defects of graphene can be calculated with $k^{o}_{obs}$ determined from the Nicholson method[42] (eqn (20) or electrochemical simulations). It is important to note that this

only works when thin-layer behaviour is not observed, as discussed below (Section 2.3.5).

Such an approach allows the global coverage of the edge plane sites/defects (% edge ($\Theta_{edge}$)) for graphene modified electrodes to be readily deduced, which can also be extended for CNTs and other graphitic materials where their electrochemical activity is due to edge plane sites.[64] Note in this case it is important to ensure that the electrode surface is completely covered to neglect the contribution from the underlying electrode, yet one must avoid thin-layer behaviour (see below). Another approach rather than using cyclic voltammetry is to use capacitance measurements but this will require a thorough understanding of capacitance and access to the correct (additional) equipment.

**2.3.5. Understanding thin-layer effects.** As mentioned above in Section 2.3.4, the procedure is valid as long as thin-layer behaviour is not observed. It is illuminating to consider what this means exactly and how this could impact the interpretation of graphene electrochemistry.

The Randles–Ševćik equations describe the electrochemical process under that of purely diffusional control such that if one performs an experiment with a redox probe and varies the voltammetric scan rate, a plot of the corresponding peak current *versus* the square root of the applied scan rate should yield a linear response. If a plot of $Log_{10}$ $I_P$ *versus* $Log_{10}$ $\nu$ is constructed, a gradient of 0.5 or close to that should be observed indicating that the response is governed by the appropriate Randles–Ševćik equation and is purely diffusional. Conversely, for a "*n*" electron reversible surface bound process, the peak current ($I_P$) may be described by the following equation:

$$I_P = \frac{n^2F^2}{4RT}\nu A\Gamma \qquad (33)$$

where $\Gamma$ is the surface coverage of the surface bound process (mol $cm^{-2}$). In this case, a plot of $Log_{10}$ $I_P$ *versus* $Log_{10}$ $\nu$ will yield a gradient of 1, as is evident from eqn (33). In this regime the modified surface, as has been shown for CNTs, exhibits a porous surface where 'pockets' of the electroactive species are trapped in-between multiple layers of nanotubes and the trapped species act akin to that of a thin layer cell.[65] The porous nanotube layer has a large surface area and the electrode is thought to be in contact with a finite, 'thin-layer' of solution (the species is trapped within the nanotube structure).

Experimentally, a transition between these two diffusional environments (thin-layer to diffusional) will be observed as the amount of material immobilised upon the electrode surface is varied (increased/decreased respectively). A key feature is the misinterpretation of experimental data due to the immobilised nanomaterial upon the electrode surface as highlighted by Compton and co-workers.[65a] As thin-layer dominates, the $\Delta E_P$ changes from diffusional to that of thin-layer such that the peak separation decreases giving the misleading impression that a material with fast electron transfer properties is giving rise to the response. In fact, as one moves towards the case of thin-layer from that of purely diffusional, the mass transport characteristics are changed such that one is misled into thinking that the reduction in peak-to-peak voltage separation is due to an electro-catalytic effect of the material![44,65b]

Care needs to be taken when adsorbing species are being explored as this will also give rise to thin-layer type voltammetry.[65c] Indeed the distinction between thin-layer diffusion and adsorption effects is not easy to make, especially in cases where the adsorption is rapidly reversible. Where there is slow adsorption (and desorption) kinetics then the presence or absence of "memory effects" can be useful. If it is possible to transfer the electrode, after exposure to the target solution, to a fresh electrolyte containing no analyte, then adsorption effects can be inferred if voltammetric signals are retained or if signals increase steadily over a period of time.[65a]

Returning to the case of graphene, it has been shown through the use of well characterised redox probes (so that adsorption is neglected) that graphene does not appear to exhibit thin-layer effects.[43] However, given the variability of graphene-type material available and with new varieties being produced by Materials Scientists, such effects still need to be considered. If thin-layer does occur, recent studies by Guo *et al.*[66] show that this can be interpreted using the classical technique of rotating disc electrochemistry; clearly thin-layer behaviour is observed with this unique (electrochemically reduced) 'graphene' which is substantially multi-layered and disordered.

**2.3.6. Electrochemical characterisation of graphene oxide.** GO has been known to exist since 1859, it constitutes single atomic layers of functionalised (oxygenated) graphene that can readily extend up to tens of μm in lateral dimension. GO can be viewed as an unconventional type of soft material as it carries the characteristics of polymers, colloids, membranes and is an amphiphile.[67] As highlighted in Section 1.1 a common approach to fabricate graphene is to chemically, thermally or electrochemically reduce GO to graphene.[8,24] The cyclic voltammetric response of GO is unique which can thus be used to ensure that GO has been fully transformed to graphene by exploring the voltammetric response before and after the chosen treatment has been applied.[68] The voltammetric response of GO using the outer-sphere redox probe hexaammine–ruthenium(III) chloride is depicted in Fig. 17A. It can be readily observed that unique voltammetry is evident, quite different to that observed at graphene (Fig. 17B)[51] and in Fig. 14B, where it is thought that in the case of GO the oxygenated species present contribute to a catalytic process, the EC' reaction, where a first 'electron transfer process' (E process), as described generally as:[68]

$$A + e^- \rightleftharpoons B \text{ (E Step)} \qquad (34)$$

is then followed by a 'chemical process' (C process) involving the electro-generated product, B, which regenerates the starting reactant, A, as described by:[68]

$$B + C \xrightarrow{k} A + \text{Products (C Step)} \qquad (35)$$

The voltammetric response arises as the amount of C is increased (the oxygenated species in this case, see Fig. 17A and ref. 68).

Note that this response is unique to hexaammine–ruthenium(III) chloride and also occurs to a lesser extent for

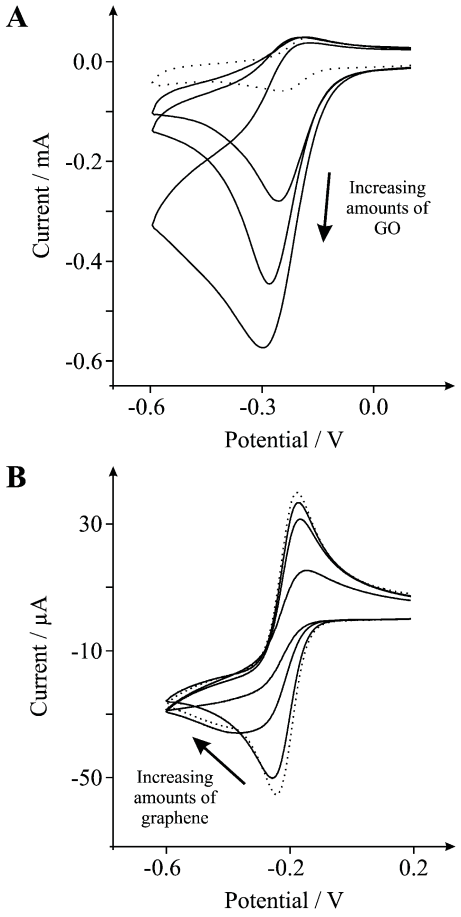


**Fig. 17** Cyclic voltammetric profiles recorded towards 1 mM hexaammine-ruthenium(III) chloride in 1 M KCl. Scan rate: 100 mV $s^{-1}$ (*vs.* SCE). A: obtained using an EPPG electrode (dotted line) after modification with increasing depositions of 1.38, 2.75 and 8.25 µg GO (solid lines). Reproduced from ref. 68 with permission of The Royal Society of Chemistry. B: Obtained using an EPPG electrode (dotted line) with the addition of increasing amounts of 100, 200 and 300 ng graphene (solid lines). Reproduced from ref. 51 with permission of The Royal Society of Chemistry.

potassium hexachloroiridate(III).[68] Owing to the contrasting behaviours of these materials, such unique and intriguing voltammetry can be used (as a characterisation technique) to provide insights into whether GO has been (successfully/fully) reduced to graphene prior to its application in a plethora of areas.[68] Also of note is work by Zhou *et al.*[69] who have reported the electrochemical reduction of GO films which has resulted in a material that has a low O/C ratio, which proceeds *via* the following electrochemical process: GO + $a\mathrm{H}^+$ + $be^-$ → ER–GO + $\mathrm{H_2O}$ (where ER implies electrochemically reduced). Of importance here is that the electrochemical reduction gives rise to reduction waves at highly negative potentials. This coupled with the observed voltammetry reported in eqn (34) and (35) could be used as a measure to determine whether GO has been efficiently (electrochemically) reduced.

**2.3.7. Electrochemical characterisation of CVD grown graphene.** The electrochemistry of CVD fabricated graphene can yield beneficial insights into the surface structure of the grown graphene layer.[70] Recently it has been demonstrated that through the careful choice of redox probes, differing voltammetric performances can be observed and insights gained regarding the structure and composition of the surface under investigation.[70]

In the case of the outer-sphere redox probe hexaammine–ruthenium(III) chloride a typical peak shaped cyclic voltammetric profile is observed and would indicate that a uniform 'graphene' film has been successfully fabricated. Of course, adequate control experiments need to be performed when characterising this material such that the electrochemical probe under investigation should also be diligently tested/performed using the underlying metal surface that the graphene has been grown upon, typically nickel[71] or copper.[37,72] This is because a non-continuous film of graphene may have been produced and the underlying metal surface upon which the graphene was grown might be exposed to the solution.[70] In this case, the underlying metal surface will act like an electrode and if the metal has favourable electrochemical properties towards the electrochemical analyte which is of interest, it will contribute to the observed electrochemical response or even dominate it, misleading researchers into thinking that graphene exhibits excellent electrochemical properties.[70] The key to determining this is to run control experiments, that is, perform the same voltammetry using the underlying supporting material (*viz* no graphene) to determine the extent of the electrochemical activity. Returning to the case of the graphene modified surface, note that if grain boundaries exist, and by this we mean that the underlying substrate is exposed to the solution due to the graphene surface not being entirely continuous, it is highly likely that the exposed material will dominate the electrochemical performance (of course this depends on the respective electron transfer kinetics of the heterogeneous electrode towards the target analyte). Again, how can one determine if this is the case? Control experiments as highlighted above should provide insights. Depending on the extent of the exposure, we expect, if for example the underlying surface is copper, copper nanobands or microbands will be realised and depending on the electrochemical activity of the exposed material, the heterogeneous surface might exhibit two voltammetric peaks (see Section 2.2); a first peak arising from fast electron transfer and a second peak from the graphene surface (which as shown in Section 2.3.1 and ref. 51 exhibits slow electron transfer rates). The extent of the observed voltammetry will depend on the electrochemical activity of the two materials comprising the heterogeneous surface, the distance between active sites (diffusion zones), voltammetric scan rates, the diffusion coefficient of the electroactive target/analyte and the coverage of the dominant electrochemically active material.

Returning to the case of the voltammetry at the CVD graphene surface, if the redox probe is changed to an inner-sphere probe such as potassium ferrocyanide, it is possible that a completely different voltammetric response is observed. Fig. 18 shows a representation of these responses. It is well documented that potassium ferrocyanide is highly surface sensitive and exhibits a response dependent upon the carbon–oxygen surface groups ranging from detrimental to beneficial responses.[56] In the case of CVD grown graphene, a sigmoidal

 

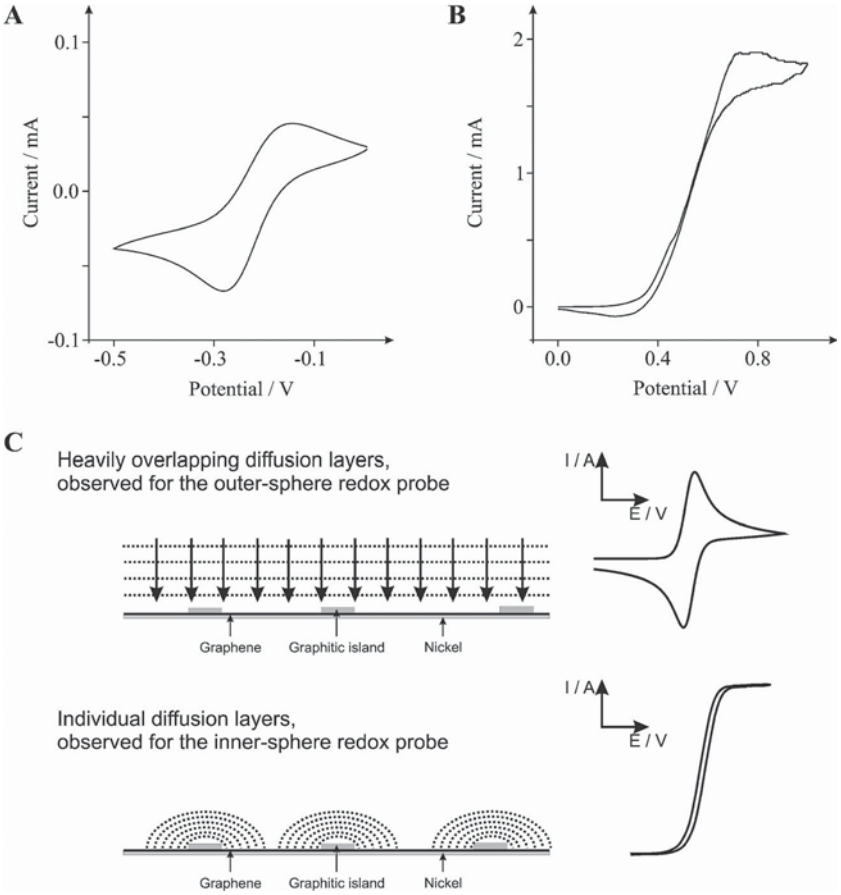


**Fig. 18** A: Cyclic voltammetric profiles recorded utilising 1 mM hexaammine-ruthenium(III) chloride in 1 M KCl, obtained using a CVD-graphene electrode (dashed line). B: Cyclic voltammetric profiles recorded for 1 mM potassium ferrocyanide(II) in 1 M KCl using a CVD-graphene electrode. C: A schematic representation of differing diffusion zones observable towards graphitic islands present upon CVD-graphene. A and B performed at a scan rate of 100 mV $s^{-1}$ (*vs.* SCE). Figure reproduced from ref. 70*a* with permission of The Royal Society of Chemistry.

voltammetric response is observed towards potassium ferrocyanide, quite different to that seen for hexaammine–ruthenium(III) chloride.[70] This is because only a certain number of graphitic domains, that is, double, few and multi-layered graphene, residing on the surface are activated with the correct proportion of carbon–oxygen groups (the carbon on the edge of graphene is hydrogen terminated) which are far from each other (separated) such that diffusion zones do not interact and thus sigmoidal voltammetry is observed.

The surface sensitivity of electrochemistry highlights that Materials Scientists can beneficially utilise electrochemistry as a tool to assist in the characterisation of their fabricated material and are thus able to differentiate between the fabrication of a continuous graphene film and a graphene film on which random multi-layered graphitic domains reside.

## 3. Pertinent applications

Fundamental electrochemical studies have aided the acquisition of an improved knowledge and understanding of many scientific principals and theories.[44] Of equal importance is the utilisation of electrochemistry within a plethora of industrial, medical and academic applications.[44] Most prominently, electrochemistry has widespread implications in the fabrication of sensing devices that have global ramifications in terms of the detection of substances harmful to human health and the environment,[9] and has further relevance in both energy production and storage devices that are of vital significance given the increasing demand for greener energy related devices with high power output and efficiency.[73]

In terms of the performance obtained from a given electrochemical device, it is the properties of the electrode material itself that are most significant. It is therefore imperative that research be conducted into the utilisation of various electrode materials (such as graphene). As stated above, graphitic forms of carbon in particular have widespread use as disposable electrode materials due to their relatively economical and simplistic fabrication processes, in addition to their non-toxic and highly conductive attributes.[11] Graphene is no exception to this trend, where owing to the combination of its interesting electrochemical properties (Section 2.3) and its reported unique assortment of physiochemical properties (see selected reviews: ref. 8–10), it has enormous potential to be beneficially utilised in a range of sensing and energy related electrochemical applications.

Within the following section we depict a concise overview and offer constructive insights and acuity into electrode design and development where graphene has been utilised

either beneficially or detrimentally within select electrochemical devices.

### 3.1. Sensing applications

The beneficial implementation of graphene as an enhanced sensor substrate has been widely reported, encompassing the detection of a diverse range of analytes including numerous bio-molecules, gases and miscellaneous organic and inorganic compounds.[9] As such there are a large number of in-depth reviews available for further reading concerning the electrochemical sensing applicability of graphene: ref. 9, 33 and 74.

**3.1.1. Direct electro-catalysis.** The "electro-catalytic" behaviour and enhanced analytical performance of graphene and related structures has been widely reported, for example towards the detection of bisphenol A,[75a] cadmium,[75b] dopamine (DA),[75c] hydrazine,[75d] morphine[75e] and vanillin[75f] to name a few. It is interesting to note that in the above examples (and in many others) the electro-catalysis of graphene is compared only to the underlying electrode (usually Glassy Carbon, GC) and not to other relevant graphitic materials, such as HOPG, graphite or GO.[9] This is a significant issue given that in the majority of studies the graphene utilised is of multi-layers (for example, 4–6+ layers),[76] which is theoretically approaching the structural composition of graphite. Additionally, where graphene modification is performed *via* liquid dispersion (as described in Section 1.1) this leads to uncertainty in terms of the coverage, orientation and quality of the graphene on the electrode surface with the possible formation of layered/disordered graphene structures – as we have observed in previous sections, such graphitic structures can contribute significantly to the observed electrochemical response and could be the *true* origin of the observed electro-catalysis, *not* graphene. Note that as highlighted in Section 2.3.2 similar misconceptions were found to be present in instances where surfactant contaminated graphenes were utilised and thus appropriate control experimentation is required.[62] As is evident in Fig. 19A, in one such recent study[77] a graphene (synthesised *via* the reduction of GO) modified GC electrode has been shown to possess excellent electro-catalytic activity towards the detection of kojic acid in terms of exhibiting a reduced over-potential and a significantly increased peak current when compared to a graphite modified alternative and the unmodified GC electrode; such data is inferred to provide a greatly improved sensing capability at the graphene fabricated electrode. However, although graphite controls were reported, the authors failed to perform appropriate control experiments with GO and thus the role of oxygenated species that may reside on the reduced GO is not clear in this case and as such may contribute significantly to the observed electro-catalysis.[77] Fig. 19B highlights other similar work towards the detection of APAP where this may also be the case.[78] In this second example the electro-catalysis of immobilised graphene (synthesised *via* GO reduction) was claimed when compared only to the response of the underlying GC electrode *viz* improvements in the observed voltammetry; such as a reduction in the $\Delta E_P$ (lower over-potential oxidation) indicating a shift from an irreversible to a quasi-reversible redox process and a dramatically increased peak current.[78] Here, due to the lack of diligent control experiments the true origin of the claimed 'electro-catalysis' is unclear given that contributions may arise from incomplete reduction of the GO or through graphitic impurities formed as a result of the fabrication process which also can contribute to a highly disordered and porous graphene structure – in which case it is likely that the observed response is due to 'thin-layer' effects (see Section 2.3.5) and the large background current exhibited by the graphene modified electrode can be attributed to the large accessible surface area of such a porous surface. Thus, the two examples highlighted above illustrate further issues regarding the need to employ appropriate control experimentation when studying *Graphene Electrochemistry*. The majority of graphene used in electrochemistry is produced through the reduction of GO, which results in partially functionalised graphene sheets or chemically reduced GO (see Section 1.1). Graphene produced in this manner usually has abundant structural defects (edge plane like-sites/defects)[25,33] and remaining functional groups which have been shown to greatly influence the electrochemical performance of the graphene fabricated device in terms of heterogeneous electron transfer rates (as is observed in Section 2.3.1) and can be either advantageous or detrimental towards the sensing of a target analyte.[9,11,45,56]

Although there are many encouraging examples of the reported 'electro-catalysis' of graphene, where improved sensitivity and detection limits have been obtained, it is evident that in the majority of cases the electrochemical performance of *true* graphene is yet to be reported and it is vital that appropriate control and comparison experiments are performed (with graphite, GO and other possible interferents/impurities (such as surfactants/solvents and those incorporated through the fabrication process))[51,62,63,68] prior to the beneficial electro-catalysis of graphene being *incorrectly* reported!

For the case of *true* graphene modified electrodes, note that the utilisation of pristine graphene has recently been explored as a potential electrode material towards the electroanalytical sensing of DA, uric acid (UA), APAP and *p*-benzoquinone.[79] To allow the true electroanalytical applicability of graphene to be de-convoluted and thus to investigate the full-implications of employing graphene in this electrochemical context, HOPG electrode substrates that exhibited either fast or slow electron transfer kinetics (EPPG or BPPG electrodes respectively) were modified with well characterised commercially available graphene that was free from surfactants, had not been chemically treated and had an extremely low oxygen content ($<5\%$).[79] Interestingly, it was observed that the graphene modified electrodes exhibited a reduced analytical performance in terms of sensitivity, linearity and the respective detection limits towards each of the analytes studied when comparison to the unmodified underlying electrode substrates (constructed from graphite) was sought;[79] as is readily observed in Fig. 19C and D for the case of DA, where increments in the over-potential are evident at the graphene modified electrodes when compared to the graphite alternatives and significantly lower peak heights (currents) reside.

This 'reduced performance' is clearly contradictory to the majority of current literature reports which claim that the application of graphene leads to an enhancement in the

 

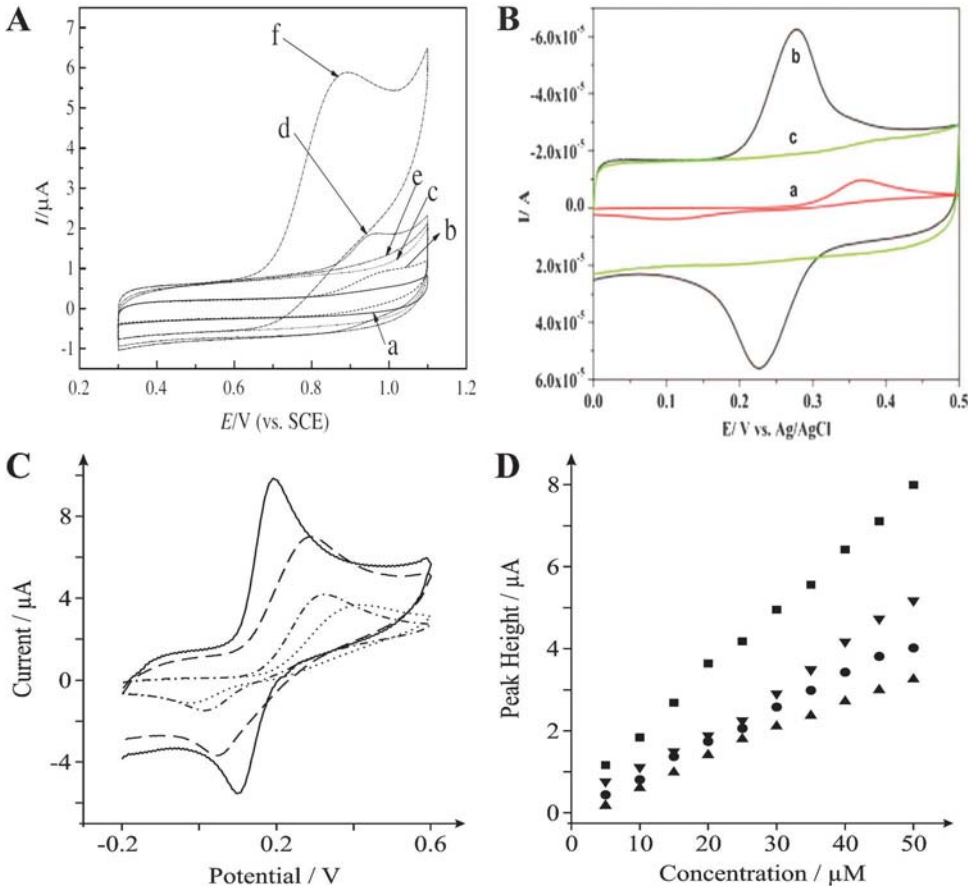


**Fig. 19** A: Cyclic voltammograms at (a and b) the bare/unmodified GC electrode, (c and d) the graphite electrode, and (e and f) the graphene/GC electrode in 0.2 M acetic acid – sodium acetate solution (pH 6.0) (a, c, and e) in the absence and (b, d, and f) in the presence of 200 μM kojic acid. Scan rate: 100 mV $s^{-1}$. Reprinted from ref. 77 with permission from Elsevier. B: The electrochemical sensing of 100 μM APAP at an unmodified GC electrode (a); and the sensing of 20 μM APAP at a graphene modified GC electrode (b), and without APAP (c) in the buffer of 0.1 M $NH_3$–$NH_4Cl$, pH 9.3, scan rate; 50 mV $s^{-1}$. Reprinted from ref. 78 with permission from Elsevier. C: Cyclic voltammetric profiles recorded for 50 μM DA in pH 7 phosphate buffer solution (PBS) using unmodified EPPG (solid line) and BPPG (dot-dashed line) electrodes, and 20 ng graphene modified EPPG (dashed line) and BPPG (dotted line) electrodes. D: Calibration plots towards the detection of DA depicting the peak height as a function of concentration, obtained *via* cyclic voltammetric measurements performed using unmodified EPPG (squares) and BPPG (circles) electrodes in addition to EPPG (inverted triangles) and BPPG (triangles) electrodes following modification with 20 ng graphene. C and D were obtained at a scan rate of 100 mV $s^{-1}$ (*vs.* SCE) – reproduced from ref. 79 with permission of The Royal Society of Chemistry.

electroanalytical response in many instances.[75–78] However importantly, such poor performances were evident at both the EPPG (fast electrode kinetics) and BPPG (slow electrode kinetics) graphene modified electrodes and, in accordance with fundamental theory (see Section 2.3), is as expected given the insights gained from earlier work utilising identical pristine graphene modified graphitic electrodes.[51,79] As mentioned in Section 2.3.1 graphene has a high electron density around its edge as opposed to its centre, where owing to its unique geometry graphene possesses a low portion of edge plane like-surface area and resultantly exhibits slow heterogeneous electron transfer kinetics, particularly when compared to its closest counterpart – graphite.[51] Thus the response observed above can be attributed (in both cases) to the relative coverage of available edge plane sites (electroactive sites) on a given electrode surface, where through the introduction of graphene the number of these sites is significantly reduced, which are replaced instead with the relatively inactive pristine basal plane sites of graphene which result in a 'blocked' electrode surface and hence reduced electron transfer kinetics. As a result a change in the overall reversibility/irreversibility of the electrode kinetics is observed (which is related to the analytical signal, $I_P$, see eqn (21) and (22));[79] note that where large deviations in the analytical signal occur it is inferred that this is due to the inherent lack of oxygenated species on the pristine graphene that are readily present upon HOPG surfaces (depending on pre-treatment of the electrode surface) and are beneficial in some instances.[56*d*,*e*,79]

Further studies concerning the application of graphite electrodes modified with pristine graphene towards the detection of heavy metals reveal identical insights as observed above.[80] It was concluded that graphene inhibits the electroanalytical sensing of cadmium(II) ions *via* anodic stripping voltammetry, with increasing additions of graphene immobilised on the electrode surface resulting in a further decline in the analytical performance and reproducibility when contrasted to that of the unmodified (graphite) electrode.[80] It is well known that metals nucleate exclusively on edge plane sites

of graphitic materials[14,44] and hence it was logically assumed that this is the case for graphene and due to the low edge to basal surface area ratio of the graphene structure, as compared to the underlying graphite electrode, the poor voltammetric response when graphene is introduced was understood to be due to graphene's low edge plane content and resultantly slow electron transfer kinetics.[51,80]

Furthermore, note that in support of the above two studies, this same trend was also found to be the case in earlier work towards the detection of hydrogen peroxide at surfactant adsorbed/contaminated graphene modified electrodes.[62c] Through careful control experimentation utilising various surfactant and graphite modified electrodes it was concluded that the graphite modified electrode exhibited a superior electrochemical response due to its enhanced percentage of edge plane sites when compared to that of graphene; sensitivities were measured at 32.8 and 49.0 μA $mM^{-1}$ for graphene and graphite modified electrodes respectively.[62c] Interestingly however, when Nafion™, routinely used in amperometric biosensors, was introduced onto the graphene and graphite modified electrodes, re-orientation was observed to occur in both cases which proved beneficial in the former and detrimental in the latter due to alterations in the availability/accessibility of each materials respective edge plane sites.[62c]

Note that important work by Pumera *et al.*[81] has emerged which demonstrates that single-, few-, and multi-layer graphene does not provide a significant advantage over graphite microparticles in terms of sensitivity, linearity and repeatability towards the electro-analytical detection of UA, where sensitivities of 4.65 and 5.11 μA $mM^{-1}$ were recorded for graphene and graphite modified electrodes respectively.[81a] These findings were later extended with regards to the electrochemical detection of 2,4,6-trinitrotoluene (TNT) where a graphite-microparticle modified electrode was shown to provide enhanced electroanalytical sensitivity when compared to the performance of single-, few-, and multi-layer graphene alternatives.[81b]

It is evident that due to graphene's structural composition (and consequently slow heterogeneous electron transfer rates, see Section 2.3.1), there appears to be no advantages of employing pristine graphene in this electroanalytical context, that is, in the case of the analytes covered here or where fast electrode kinetics are imperative with respect to enhanced and beneficial analytical performances. It must be noted that within these select studies the EPPG electrode consistently exhibited the best performance owing to its favourable orientation of the graphite planes resulting in optimum edge plane coverage (and in certain cases the presence of oxygenated species),[51,70b,79,82] which questions the need to modify electrodes with graphene for the electroanalysis of target analytes in the first place; however, see later.

It should be remembered however, that graphene-based nanomaterials can differ significantly if different methods of preparation are used or even if small variations of a single method are employed.[34] Therefore, any graphene nanomaterial should be thoroughly characterised to avoid potential misinterpretation.[21] Furthermore, as touched upon in Section 2.3.1 this allows the effective manipulation and tailoring of the electrochemical properties of graphene for specific applications; thus if the orientation of graphene was controlled/manipulated to give rise to a large degree of accessible edge plane like-sites/defects, one would expect to observe an improved performance in terms of electroanalysis (see Section 3.1.2 for examples where this is the case).

With the above insights in mind, Brownson *et al.* have recently explored and contrasted the electroanalytical performance of a commercially available CVD grown graphene electrode to that of EPPG and BPPG electrodes constructed from HOPG for application towards the sensing of biologically important analytes, namely NADH and UA.[82] Utilising cyclic voltammetry the analytical sensitivities observed towards the detection of NADH at CVD graphene, EPPG and BPPG electrodes were 0.26, 0.22 and 0.15 A $cm^{-2}$ $M^{-1}$ respectively.[82] The similar responses observed at the EPPG and CVD graphene electrodes was inferred to be due to the similar electronic structures of the electrode surfaces (global coverage of edge plane sites, where similar coverages at CVD graphene and EPPG was confirmed *via* AFM given that the CVD graphene surface was highly disordered in nature with graphene orientated both parallel and perpendicular to the surface in addition to the prevalence of graphitic islands across its surface which contribute to a large global coverage of edge plane sites – Fig. 20 depicts an AFM image of the CVD graphene surface, which is known to be polycrystalline, highly disordered and defect abundant when grown on nickel substrates, see ref. 34), in which case the enhanced performance of the CVD graphene over that of the BPPG electrode is as expected given the former possesses a greater degree of edge plane sites over the latter (as would an EPPG electrode).[82] Interestingly, for the case of UA the analytical sensitivities of the CVD graphene, EPPG and BPPG electrode were 0.48, 0.61 and 0.33 A $cm^{-2}$ $M^{-1}$ respectively, where notably although the performance of the CVD graphene electrode surpassed that of the BPPG electrode it was inferior to that observed at the EPPG electrode, which was inferred to be due to UA's respective surface sensitivity towards the (favourable) presence of oxygenated species and thus was indicative of the differing O/C ratios at the two electrodes.[56e,70b,82] It is clear that for the analytes studied, in the best case, the electroanalytical performance of the CVD graphene electrode mimicked that of EPPG, again suggesting no significant advantage of utilising CVD graphene in this analytical context.[82]

The above work highlights the importance of edge plane sites (and the respective orientation of graphene sheets) and oxygenated species (either their absence or presence) in electroanalysis,[82] where control of these factors has the potential to lead to the development of enhanced analytical sensors. For example, for graphene to be utilised beneficially in electroanalysis it is becoming evident that one must be able to control 'with atomic precision' the size, shape and orientation of the graphene sheets upon a supporting substrate (edge plane favourable stacking, or the production of nano-ribbons with high edge plane to basal plane surface area ratios), the degree of defect density across the basal plane of the graphene sheets (where more defects are beneficial for electrochemical electron transfer mechanisms), the degree of functionalisation (where specific oxygenated species are either beneficial or detrimental) and finally control over the vast array of unique physicochemical properties that must be utilised in their entirety

 

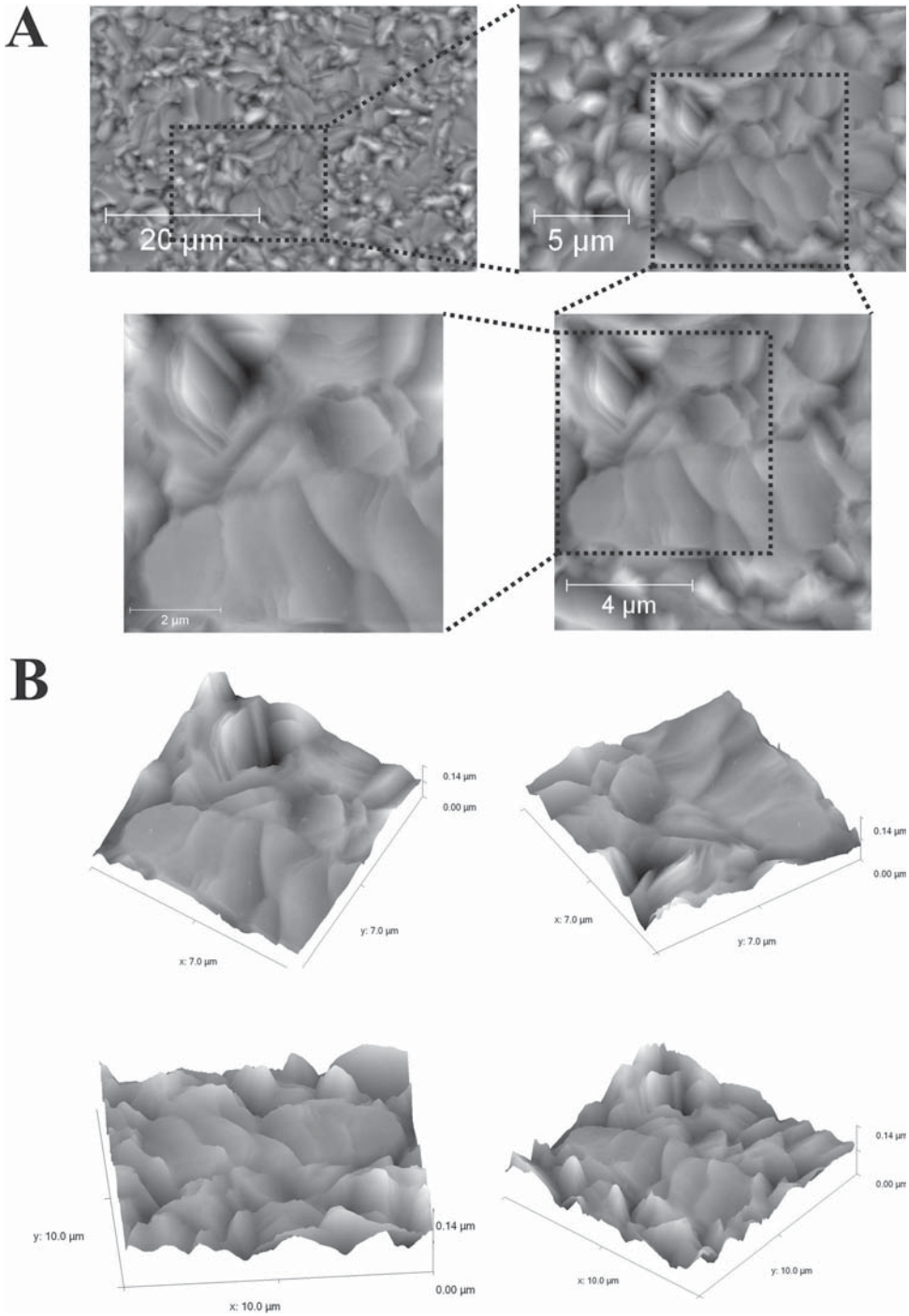


**Fig. 20** AFM images of the 'as received' commercially available CVD graphene surface, observed from various top-down (A) and three-dimensional (B) perspectives. Note that the surface is generally akin to that of a HOPG surface, but is highly disordered and thus as a result there is a high edge plane content making the two electrodes in comparison act electrochemically similar. Reproduced from ref. 82 with permission of The Royal Society of Chemistry.

(beneficial surface area, optical transparency, flexibility and the possible doping of pristine graphene to name a few).

It is evident that if true graphene is employed in the context covered above (where fast electron transfer is beneficial), the best response that can be achieved is that akin to an EPPG electrode, that is, as governed by the Randles–Ševćik equations; any deviation from this results from either thin-layer behaviour (Section 2.3.5) or could possibly be due to changes in mass transport characteristics or other contributing factors (as discussed above) rather than (wrongly) assigning the graphene to be 'electro-catalytic'.

**3.1.2. Miscellaneous sensing applications.** So far, pristine graphene is yet to be realised as a beneficial sensing material in electroanalysis. It is clear from inspection of the above Section 3.1.1 that one must seek to take advantage of

graphene's various physicochemical properties or manipulate and control its electrochemical properties in order to realise the true potential of this novel material.

One particular property of graphene that has potential to be useful is its large basal plane proportion and insights from fundamental work on graphitic electrodes can be applied where graphene is utilised.

Recently Compton *et al.*[83] have thoroughly investigated the electrochemical detection of the DNA bases adenine and guanine at graphitic electrodes. The case of adenine is particularly interesting as the peak current, studied as a function of scan rate at low concentrations, was found not to vary linearly with either the square root of the scan rate or with the scan rate as would be expected for a diffusional or adsorptive process; a plot of $I_P/\nu^{0.5}$ *versus* $\nu^{0.5}$ was found to give a straight line. This suggests that the peak was a result of both diffusion and adsorption factors. The equation of a surface bound species is given by:

$$I_{SBS} = \frac{n'\theta F^2}{2.718RT}\nu A\Gamma \quad (36)$$

where $I_{SBS}$ is the peak current for a surface bound species involving multiple electrons and a chemically irreversible process, $n'$ is the number of electrons transferred prior to the chemically irreversible step, and $\theta$ is the total number of electrons transferred in the redox process divided by $n'$.[83] Note that the denominator has changed from 4 in eqn (33) to 2.718 in eqn (36) reflecting the chemical step in the electrochemical mechanism; this form of the equation is comparable to that found for an irreversible surface bound species.[44] In this case, the peak current for a multi-electron diffusion-only process involving a chemically irreversible step is given by:

$$I_{DS} = (2.69 \times 10^5)AD^{0.5}C^*\nu^{0.5}n'^{1.5}\theta \quad (37)$$

where $I_{DS}$ is the peak current for a diffusional species. Note that this only holds if the chemical step is fast and irreversible and the electron transfer prior to the chemical step does not have a standard potential more than approximately 200 mV greater than that of the first electron transfer. Hence the following equation describes the observed peak current for the oxidation of a low concentration of adenine at pH 6.85 at an EPPG electrode, where it is assumed that the two processes occur in parallel:

$$I_P = I_{DS} + I_{SBS} \quad (38)$$

where the first term is related to the peak current for the diffusional process (eqn (37)) and the second term is related to that of the adsorbed species (eqn (36)). Assuming that the surface coverage, $\Gamma$ of the target analyte exhibits a linear dependency on the concentration, $C^*$ of the analyte under investigation, and assuming a simple adsorption isotherm which, one can write $\Gamma = KC^*$ which is only valid for low bulk concentrations (where $K$ is an experimental constant).[83] At higher concentrations a more complex analysis is required and additionally if inhibition of the surface occurs it would not be possible to measure a response at all.[83] Eqn (38) leads to;

$$I_P = (2.69 \times 10^5)AD^{0.5}C^*\nu^{0.5}n'^{1.5}\theta + \frac{n'\theta F^2}{2.718RT}\nu AKC^* \quad (39)$$

This equation shows that for the case of adenine, basal plane sites are responsible for adsorption (second part of the equation) and edge plane sites are responsible for the electrochemical oxidation (first part of the equation). Thus in terms of pristine graphene, the large proportion of basal plane sites would give rise to many adsorption sites of adenine and the edge plane sites would produce the analytical signal. Recently this has indeed been shown to be the case for pristine graphene but due to the low proportion of edge plane sites arising from the unique structure of graphene, the electrochemical signal was found to be relatively small precluding its use for the basis of an electrochemical sensor;[84] a more advantageous approach would be to use graphene with more edge plane like-defects across the surface of its basal plane. Interestingly this has recently been shown to be the case. Pumera *et al.* has studied the electroanalytical performances of chemically-modified graphenes containing different defect densities and varied amounts of oxygen-containing groups.[85] The authors showed that differences in surface functionalities, structure and defects of various modified graphenes largely influence their electrochemical behaviour in detecting the oxidation of adenine, with later work by the group demonstrating that few-layer graphene exhibits improved electroanalytical behaviour over that of single-layer graphene, multi-layered graphene (*viz* graphite), EPPG and unmodified GC electrode alternatives.[85] Importantly, this work shows how it is possible to effectively tailor graphene to exhibit a range of favourable/required characteristics/properties for beneficial implementation and this will no doubt have a profound influence on the construction of graphene based sensors.

With this in mind, Lim *et al.*[55] have reported the beneficial implementation of an electrochemically anodised CVD grown graphene electrode (which increases the degree of oxygen-related edge plane defects, and thus as reported in Section 2.3.1, exhibits improved electron transfer kinetics over that of pristine graphene) towards the electroanalysis of select bio-molecules, namely the detection of nucleic acids, UA, DA and ascorbic acid (AA). Utilising differential pulse voltammetry the authors demonstrated that mixtures of nucleic acids (adenine, thymine, cytosine and guanine) or bio-molecules (AA, UA and DA) can be resolved as individual peaks and that the anodised graphene electrode could simultaneously detect all four DNA bases in double stranded DNA (dsDNA) without a pre-hydrolysis step in addition to differentiating single stranded DNA from dsDNA.[55] Throughout their work Lim *et al.* contrasted the response of the anodised graphene electrode to that of pristine graphene, GC and BDD alternatives where the response of the anodised graphene electrode surpassed and out-perform each alternative.[55] This work shows that graphene with an elevated level of edge plane defects, as opposed to pristine graphene, is the choice platform in high resolution electrochemical sensing.

Note that in support of this work there are various reports where graphene that is highly disordered or defect abundant (high edge plane content) or of which possesses a beneficial oxygen content has been utilised advantageously within select sensing applications.[56d,86] Interestingly, while the functionalisation of graphene is deleterious to its electrical conductivity, the resulting oxygen-containing groups and structural defects

can be beneficial for electrochemistry, as these are the major sites for rapid heterogeneous electron transfer and also these sites provide convenient attachment sites in the development of nano-architectonics or the attachment/adsorption of biomolecules where specific groups can be introduced that play vital roles in electrochemical sensing and energy applications, hence the electrochemical properties of graphene-based electrodes can be modified or tuned by chemical modification and tailored to suit appropriate applications.[74]

Furthermore, it must be noted that in order to beneficially modify the inherent properties of graphene many researchers turn to the utilisation/fabrication of doped graphene structures or to graphene hybrid/composite materials which have significantly altered electrochemical properties, where modification of the graphene can result in improved conduction or electronic properties (DOS), increased disorder or edge plane accessibility and beneficial contributions in terms of the catalytic effects of the various incorporated materials.[61] Numerous studies concerning the implementation of such electrode materials have been reported, for example towards the ultrasensitive analytical detection of cocaine,[87a] hydrogen peroxide,[87b] mercury,[87c] oxalate[87d] and TNT.[87e] In one notable example Sheng and co-workers utilised a nitrogen doped graphene (NG) based electrode towards the simultaneous determination of AA, DA and UA.[88] As depicted in Fig. 21 NG shows highly electro-catalytic activity towards the oxidation of all three analytes and additionally the electrochemical sensor showed a wide linear response and low detection limits for AA, DA and UA, attributed by the authors to be due to its unique structure and properties originating from nitrogen doping.[88] This work demonstrates that NG is a promising candidate for use as an advanced electrode material in electrochemical sensing and other electro-catalytic applications. Moreover, graphene composites have proven to be particularly promising within bio-sensing as a glucose sensor. Kang *et al.*[89] have reported the direct electrochemistry of a glucose oxidase-graphene-chitosan nanocomposite (loaded upon a GC electrode), commenting that the use of a graphene based material obtained a greatly improved enzyme loading capability than GC surfaces.[89] The authors claimed that the graphene-immobilised enzyme retained its bioactivity and exhibited a surface confined, reversible two-proton and two-electron transfer reaction, where great activity, stability and fast heterogeneous electron transfer rates were evident.[89] When compared to other nanostructured supports (including: single- and multi-walled CNTs and an unadulterated GC electrode) the fabricated bio-sensor exhibited a wide linear range of 0.08 to 12 mM and had a lower glucose detection limit of 0.02 mM in addition to a greatly enhanced sensitivity; demonstrating that a glucose oxidase-graphene-chitosan nanocomposite film can be used as a sensitive and effective glucose detection strategy, with potential for graphene based glucose bio-sensors for clinical diagnosis in the future.[89]

Given the above insights, it is clear that once one can successfully alter and manipulate the inherent properties of graphene, it does appear to be a promising platform on which potential enhancements will no doubt develop – providing ultrasensitive graphene based sensors for a wide range of important analytes in the future. That is of course once the appropriate control experimentation has been performed and diligently reported so that a clearer understanding of the observed response can be attained and the misinterpretation of experimental data is avoided. Caution is also advised with the possible limitations in mind relating to the reproducibility, scalability and appropriate characterisation of graphene based electrochemical sensing devises – these issues should also be born in mind and applied within the next Section 3.2 with regards to the application of graphene and related structures in energy production and storage devices.

### 3.2. Energy storage and generation applications

The beneficial implementation of graphene as an enhanced energy storage and generation electrode material has been widely reported.[73] Energy generation and storage devices are inundated with both environmental and performance related issues, where increasing demands for the improved portability, energy efficiency, and power output of capacitors, batteries, fuel cells and solar cells constitute immense research interest.[73] As a result there are a large number of in-depth reviews available for further reading concerning the applicability of graphene in electrochemical energy related devices: ref. 73, 90 and 91.

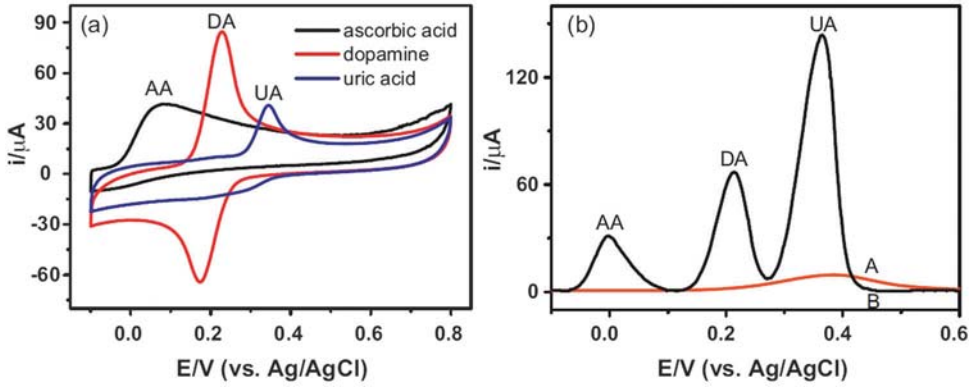


**Fig. 21** (a) Cyclic voltammograms of 1.0 mM AA, 1.0 mM DA and 1.0 mM UA in 0.10 M PBS (pH 6.0) at NG modified GC electrode at a scan rate of 100 mV $s^{-1}$. (b) Differential pulse voltammograms for 1.0 mM AA, 0.05 mM DA and 0.10 mM UA in a 0.1 M PBS (pH 6.0) at a bare GC electrode (A) and a NG/GC electrode (B), respectively. Reprinted from ref. 88 with permission from Elsevier.

**3.2.1. Energy storage devices: super-capacitors.** Electrochemical super-capacitors are passive and static electrical energy storage devices that find application in portable electronics, memory back-up systems and hybrid cars, where extremely fast charging is a valuable feature.[73,91d] In super-capacitor devices energy is stored either due to the formation of an electrical double layer at the interface of the electrode and the electrolyte (electrical double layer capacitor (EDLC)) or due to electron transfer between the electrolyte and the electrode through fast Faradiac redox reactions (pseudo-capacitor).[73] For super-capacitors the ability to utilise both of the previous energy storage capabilities with high efficiency, where these two mechanisms can function simultaneously depending on the nature of the electrode material, is often the capacitance determining factor.[73] Current research on electrochemical capacitors is focused on increasing the power and energy densities of fabricated devices, as well as lowering fabrication costs whilst incorporating environmentally friendly materials.[73]

Numerous reports have emerged where graphene has been utilised as an independent super-capacitor material for EDLCs.[92,93] According to the EDLC energy-storage mechanism, the key to enhancing specific capacitance is to enlarge the specific surface area and control the pore size, layer stacking and distribution of the electrode material.[73] In one notable study Du *et al.*[94] mass-produced graphene nano-sheets with a narrow mesopore distribution of $\sim$4 nm from natural graphite *via* oxidation and rapid heating processes finding them to maintain a stable specific capacitance of 150 F $g^{-1}$ under the specific current of 0.1 A $g^{-1}$ for 500 cycles of charge–discharge; upon comparison to various other graphene–graphite structures this important work demonstrated that an electrode with greater disorder in the graphene stacking and with plenty of available edge plane like-sites/defects is key for the enhancement of EDLC performance. In other work Wang *et al.*[95] report a maximum specific capacitance of 205 F $g^{-1}$ with a power density of 10 kW $kg^{-1}$ at a energy density of 28.5 W h $kg^{-1}$ whilst utilising single layered graphene (produced *via* GO). Their electrode showed excellent cyclic ability, with $\sim$90% specific capacitance remaining after 1200 cycles, which far surpassed the performance obtained at a comparable graphite based alternative, demonstrating the exciting commercial potential for high performance, environmentally friendly and low-cost electrical energy storage devices based on single layer graphene.[95]

It is important to note however, that work by Pumera *et al.*[96] has shown it is not always beneficial to exfoliate graphitic structures to single layer graphene in order to achieve maximum electrochemical performance and capacitance. Using electrochemical impedance spectroscopy, the authors demonstrated that multi-layer ($>$10 layers) graphene nanoribbons provide a larger capacitance (15.6 F $g^{-1}$) than few-layer (3 to 9 layers) graphene nanoribbons (14.9 F $g^{-1}$) and a far greater capacitance than single layer graphene sheets (10.9 F $g^{-1}$).[96] Pumera *et al.* inferred that the graphene layers were likely laying flat (horizontal), 'on top of one another' and consequently were blocking/concealing the important edge plane sites and available surface area; the authors stated that conversely, vertically orientated graphene stacks (*i.e.* multi-layered graphene) would be a near-ideal structure due to larger inter-layer spaces allowing for improved capacitance due to the complete utilisation of available surface area and edge plane sites.[96] Interestingly, the findings of further recent studies exploring the capacitance of graphene and graphite modified electrodes can be interpreted to imply a similar connotation.[62d] Galvanostatic charge/discharge analysis was performed on both graphene and graphite modified electrodes (under identical conditions) where the specific capacitances of 62.6 F $g^{-1}$ and 5.4 F $g^{-1}$ were obtained respectively at a discharge current of 67 nA.[62d] It appears that although graphite has a larger portion of edge plane sites than that of graphene, it is a 'bulk' material where tightly stacked layering leads to the reduced accessibility of available surface area.[62d] The larger capacitance of graphene can be attributed to a combination of capacitance due to available edge plane sites and surface area, where enhanced layer spacing results in the superior accessibility of these available components in flexible graphene sheets as opposed to bulk graphite, consequently leading to the higher capacitance values observed.[62d]

Moreover, it is important to highlight the impact of surfactants and moieties on the performance of graphene based capacitors that, as within sensing applications, when present require appropriate control experiments to be performed to de-convolute the true origin the responses observed.[62d] Within the work noted above, the specific capacitance of an alternatively available commercially produced graphene (in the presence of the surfactant sodium cholate) was found to be 148.6 F $g^{-1}$ at a discharge current of 1.3 μA, which compared to 156.0 F $g^{-1}$ for the surfactant alone (no graphene) under identical conditions.[62d] It is clear that, when present, the surfactant dominates the capacitive behaviour of graphene and thus in such cases the observed response is likely from the surfactant and not the graphene, where graphene's influence (the difference) is diminutive:[62d] complementary work by Zhang *et al.* has shown that variable other surfactants also strongly influence the performance of such graphene based devices.[97] For the case of oxygenated functional species, previous literature has demonstrated that various functional groups residing at the interface of carbon particles (mainly at the edge plane) may either beneficially or detrimentally influence the resultant capacitance by affecting the wettability of the electrode and the penetration of the electrolyte, where enhanced wettability (hydrophilicity) resulted in increased specific capacitance due to a higher efficiency utilisation of surface area.[98] However, in a recent study GO was shown to exhibit a reduced performance when compared to pristine graphene and thus it was evident that in the case of the commercially purchased GO utilised, the surface groups present were likely detrimental.[62d] Note that recent key attributes to the field are in favourable agreement with the above insights, where it has been shown that increased interlayer spacing and reduced oxygen content are favourable with regards to the enhanced performance of graphene based EDLCs – where oxygen content was the main influential factor.[99]

The above studies provide valuable insights into the fabrication of graphene super-capacitors. It is clear however that the general specific capacitance of graphene is not as high as expected and thus it is notable that many researchers have turned,

 

as is the case for sensing applications, to doping graphene or fabricating graphene based hybrid materials in the pursuit of improved capacitance performance (in-accordance to the factors noted above).[73,92,100] Many hybrid materials involve combining graphene with other nanomaterials such as various metals, metal oxides, metal hydroxides and polymers as to utilise both of the energy storage mechanisms simultaneously and with high efficiency (*i.e.* obtaining energy storage through both EDLC and pseudo-capacitor contributions); see for example: ref. 92 and 100. In one notable example a novel high performance electrode material based on a graphene–polyaniline (PANI) composite has been reported by Yan *et al.*[101] where their *in situ* polymerisation synthesised composite obtained a high specific capacitance of 1046 F $g^{-1}$ (examined using cyclic voltammetry and galvanostatic charge–discharge analysis), which compared to 115 F $g^{-1}$ for pure PANI, 463 F $g^{-1}$ for single-walled-CNT–PANI and 500 F $g^{-1}$ for a multi-walled-CNT–PANI. Note also, the energy density of the graphene–PANI composite could reach 39 W h $kg^{-1}$ at a power density of 70 kW $kg^{-1}$.[101] It was inferred that graphene–PANI modifications offer a highly conductive support material where well-dispersed depositions of nanoscale PANI particles relate to high performance given graphene's flexibility and large accessible surface area. Other work on this topic[102] has investigated the effect of a graphene–CNT–PANI composite, claiming responses similar to the composites mentioned above, however excellent cyclic performance was also noted, where after 1000 cycles the capacitance decreased by only 6% of the initial compared to 52 and 67% for graphene–PANI and CNT–PANI composites respectively. Thus it is evident that a graphene-hybrid material may exhibit the ultimately desired properties required for superior energy related devices to be realised.[100–102]

**3.2.2. Energy storage devices: lithium-ion batteries.** Lithium-ion (Li-ion) batteries store and supply electricity over long periods of time, where the electrode material (*i.e.* the anode–cathode) plays a dominant role in the batteries performance.[103] Currently the anode material employed for lithium based batteries is usually graphite because of its high Coulombic efficiency (the ratio of the extracted Li to the inserted Li) where it can be reversibly charged and discharged under intercalation potentials with a reasonable specific capacity.[103] To improve battery performance the relatively low theoretical capacity associated with graphite batteries (372 mA h $g^{-1}$) and the long diffusion distances of the Li-ions need to be overcome.[73,103] Graphene's reportedly superior physical attributes suggest that it should constitute a beneficial replacement electrode material for lithium based rechargeable batteries.[73]

Graphene has been used directly as an anode material for Li-ion batteries where it has been claimed that its utilisation improved the electrochemical properties and performance of fabricated devices.[90] For example, Lian *et al.*[104] report the first reversible specific capacity of a graphene electrode to be as high as 1264 mA h $g^{-1}$ at a current density of 100 mA $g^{-1}$. After 40 cycles, the reversible capacity was retained at 848 mA h $g^{-1}$ at a current density of 100 mA $g^{-1}$, note that this is higher than general values reported at both CNT and graphite electrodes;[104] the favourable performance is most likely due to the increased flexibility and degree of accessible surface area at the graphene structure.[104] Additionally the graphene nanostructures utilised in the above study were thought to have significant disorder and defects, which as verified by comparable reports is beneficial for Li-ion storage where highly disordered graphene nanosheets exhibit high reversible capacities (794–1054 mA h $g^{-1}$) and good cyclic stability.[105] In terms of modifying the graphene as to improve its performance, work by Bhardwaj *et al.*[106] confirmed that oxidised graphene nanoribbons (ox-GNRs) outperformed CNTs and pristine graphene, presenting a first charge capacity of $\sim$1400 mA h $g^{-1}$ and a reversible capacity of $\sim$800 mA h $g^{-1}$. In this case it is likely that both the large edge plane surface area possessed by the ox-GNRs, favourable interlayer spacing (porosity, disorder) and the oxygenated species contributed beneficially towards the enhanced performance of the device in terms of favourable Li-ion intercalation.

The above work is supported by reports that show enhanced interlayer spacing, an increased availability of the surface area and fewer layers of graphene samples that are disordered/porous in nature exhibit superior characteristics for this application.[107] It is no surprise therefore that the majority of research is focused on achieving greater disorder of the graphene utilised or on enhancing these variable other contributing factors, which can be achieved *via* a variety of methods including electron-beam irradiation[105] and of course (as is the case in sensing and super-capacitors) the fabrication of hybrid graphene composite materials. A large number of graphene based composites which exhibit enhanced battery performance in terms of both the capacity and cyclic ability have been reported, these usually involve the incorporation of other polymer or metal based components.[108] However, the prevailing factor attracting scientists towards the creation of hybrid materials is to alleviate issues with rapid capacity fading during cycling at carbon based materials.[73] The most significant work in this area was by Zhou *et al.*[109] who fabricated a well-organised flexible interleaved composite of graphene decorated with $Fe_3O_4$ particles through the *in situ* reduction of iron hydroxide between the graphene sheets; the authors claim that the interleaved network of graphene sheets produce a pathway for electron transport where the accessible capacity was improved as the graphene provides a large contact surface in addition to improvements in the adsorption and immersion of the electrolyte due to the $Fe_3O_4$ particles separating the graphene sheets and preventing their restacking. The graphene–$Fe_3O_4$ composite was shown to exhibit a reversible specific capacity approaching 1026 mA h $g^{-1}$ after 30 cycles at 35 mA $g^{-1}$ and 580 mA h $g^{-1}$ after 100 cycles at 700 mA $g^{-1}$.[109] Additionally, improved cyclic stability and an excellent rate capability were evident when compared towards the capacities of bare/unmodified $Fe_2O_3$ and $Fe_2O_4$ particles (which are utilised commercially) after 30 cycles.[109]

In light of the above literature, current research regarding graphene (particularly graphene based hybrid/composite materials) as the basis for a Li-ion storage device indicates it to be beneficial over graphite based electrodes, exhibiting higher capacitance and improved cyclic performances. Once again exciting future developments in this area are expected.

**3.2.3. Energy production/generation and conversion.** With the depletion of non-renewable energy resources ever-nearing the search for replacements has resulted in great interest in fuel and solar cell applications.[73] Graphene based hybrid materials are a particularly attractive group of electrode materials for use within fuel cells because of the presence of a large surface area, improved enzymatic binding ability, unique electrical conductivity and widely applicable electro-catalytic activity (particularly in the case of metal composites where one can benefit from specific catalytic properties of various additional components) and low production costs.[26,73]

A large number of graphene based fuel cells have thus been reported in the literature, including the use of a metal free nitrogen doped graphene electrode (with respect to the oxygen reduction reaction, ORR),[110] microbial fuel cells which offer a great opportunity for cleaner, more sustainable energy whilst at the same time utilising waste products and meeting increasing energy demands,[111] enzymatic bio-fuel cells which possess the potential to be employed as an *in vivo* power source for implantable medical devices,[112] and many more examples[113] all of which boast superior operational performance in terms of electro-catalytic activity and long-term operation stability owing to the presence of graphene.

Of particular interest are direct methanol fuel cells which have drawn great attention recently due to their high energy densities, low pollutant emission, ease of handling (the liquid 'fuel') and low operating temperatures (60–100 °C), however, low electro-catalytic activity towards methanol oxidation is hindering exploitation.[73] Xin *et al.*[114] have recently linked graphene to the enhanced electro-catalytic activity of catalysts for fuel cell applications by demonstrating that the utilisation of a Pt/graphene catalyst exhibits a high catalytic activity for both methanol oxidation and the ORR when compared to Pt supported on carbon black. In further promising work Shang *et al.*[115] have investigated the application of uniform and porous graphene sheets as a support for catalytic Pt nano-clusters in direct-methanol electro-oxidation, with the authors claiming this novel graphene supported Pt based nanostructure has the potential to serve as a low-cost and highly efficient electrode material for methanol fuel cells: additionally, Soin and co-workers[116] have shown that a vertically aligned, few-layer graphene electrode (with Pt nanoparticle deposits) exhibits a high resistance to carbon monoxide poisoning (and consequential deterioration in performance) when compared to commercially available alternatives. Thus it appears that graphene is a good candidate for potential applications in the fabrication of high-energy 'greener' solutions to current issues surrounding fuel cells, particularly for use as a supporting material in high-loading metal catalyst devices once the fundamental processes for metal immobilisation onto graphene are investigated further, as currently they are not fully understood.[73]

Finally, note that graphene films have been explored as an advantageous transparent conductive electrode material for use in organic photovoltaic flexible solar cells with beneficial properties being expressed.[117] In one notable example transparent CVD grown graphene conducting films were successfully incorporated in thin-film CdTe solar cells as the front electrode.[118] The authors report the fabricated device to possess a carrier mobility of 550 $cm^2\ V^{-1}\ s^{-1}$ and an optical transparency of 90.5% from 350 to 2200 nm; achieving an overall power conversion efficiency of 4.17% in the prototype device, which is comparable to alternative carbon based devices.[117,118]

The reports highlighted in this section suggest that graphene composite materials may serve as a promising platform for high-energy 'efficient' fuel cells and solar energy conversion within the future. However, on a final note, caution is advised with regards to the appropriate control measures being performed (see earlier) and issues are expected to reside with the reproducibility and scalability of given fabricated devices.

## 4. Conclusions

In this tutorial review we have summarised the key developments in the field of Graphene Electrochemistry, first providing a basic introduction to this field before highlighting pertinent examples and finally summarising applications. Although there are many outstanding properties of graphene which are due to the low proportion of defects across the graphene surface, nano-engineering of graphene based devices is necessary to introduce structural defects or impurities that will allow the desired functionality and electronic structures to give rise to useful electrochemical activity. Additionally, this can be extended to graphene oxide where carbon–oxygen groups can be beneficial or detrimental towards the electrochemical response. As new routes to fabricate graphene are produced, in terms of electrochemistry, this article aims to aid those involved to properly characterise their material and benchmark it against other graphenes, as well as undertaking the appropriate control experiments with graphite and graphitic electrodes. Due to the array of different graphenes that can be produced and the wide application of graphene in electrochemistry, the area is truly fascinating.

## References


1 E. Fitzer, K.-H. Kochling, H. P. Boehm and H. Marsh, *Pure Appl. Chem.*, 1995, **67**, 473–506.
2 Web-Resource, *The 2010 Nobel Prize in Physics – Press Release*, Nobelprize.org. 28 Feb 2012: http://www.nobelprize.org/nobel_prizes/physics/laureates/2010/press.html.
3 K. S. Novoselov, A. K. Geim, S. V. Morozov, D. Jiang, Y. Zhang, S. V. Dubonos, I. V. Grigorieva and A. A. Firsov, *Science*, 2004, **306**, 666–669.
4 See summary by: E. S. Reich, *Nature*, 2010, **468**, 486–486.
5 K. S. Novoselov, D. Jiang, F. Schedin, T. J. Booth, V. V. Khotkevich, S. V. Morozov and A. K. Geim, *Proc. Natl. Acad. Sci. U. S. A.*, 2005, **102**, 10451–10453.
6 (*a*) P. R. Wallace, *Phys. Rev.*, 1947, **71**, 622–634; (*b*) D. R. Dreyer, R. S. Ruoff and C. W. Bielawski, *Angew. Chem., Int. Ed.*, 2010, **49**, 9336–9344; (*c*) A. K. Geim, *Phys. Scr.*, 2012, **2012**, 014003.
7 C. Soldano, A. Mahmood and E. Dujardin, *Carbon*, 2010, **48**, 2127–2150.
8 Y. Zhu, S. Murali, W. Cai, X. Li, J. W. Suk, J. R. Potts and R. S. Ruoff, *Adv. Mater.*, 2010, **22**, 3906–3924.
9 D. A. C. Brownson and C. E. Banks, *Analyst*, 2010, **135**, 2768–2778.
10 A. K. Geim and K. S. Novoselov, *Nat. Mater.*, 2007, **6**, 183–191.
11 R. L. McCreery, *Chem. Rev.*, 2008, **108**, 2646–2687.
12 T. J. Davies, M. E. Hyde and R. G. Compton, *Angew. Chem., Int. Ed.*, 2005, **44**, 5121–5126.
13 T. J. Davies, R. R. Moore, C. E. Banks and R. G. Compton, *J. Electroanal. Chem.*, 2004, **574**, 123–152.

14 C. E. Banks and R. G. Compton, *Analyst*, 2006, **131**, 15–21.
15 (*a*) M. A. Edwards, P. Bertoncello and P. R. Unwin, *J. Phys. Chem. C*, 2009, **113**, 9218–9223; (*b*) C. G. Williams, M. A. Edwards, A. L. Colley, J. V. Macpherson and P. R. Unwin, *Anal. Chem.*, 2009, **81**, 2486–2495; (*c*) S. C. S. Lai, A. N. Patel, K. McKelvey and P. R. Unwin, *Angew. Chem., Int. Ed.*, 2012, **51**, 5405–5408.
16 K. K. Cline, M. T. McDermott and R. L. McCreery, *J. Phys. Chem.*, 1994, **98**, 5314–5319.
17 M. C. Henstridge, E. Laborda, N. V. Rees and R. G. Compton, *Electrochim. Acta*, 2011, DOI: 10.1016/j.electacta.2011.10.026.
18 R. Nissim, C. Batchelor-McAuley, M. C. Henstridge and R. G. Compton, *Chem. Commun.*, 2012, **48**, 3294–3296.
19 (*a*) N. M. R. Peres, L. Yang and S.-W. Tsai, *New J. Phys.*, 2009, **11**, 095007; (*b*) R. L. McCreery and M. T. McDermott, *Anal. Chem.*, 2012, **84**, 2602–2605.
20 D. Jiang, B. G. Sumpter and S. Dai, *J. Chem. Phys.*, 2007, **126**, 134701.
21 M. Pumera, *Chem. Soc. Rev.*, 2010, **39**, 4146–4157.
22 Y. Shimomura, Y. Takane and K. Wakabayashi, *J. Phys. Soc. Jpn.*, 2011, **80**, 054710.
23 R. Sharma, J. H. Baik, C. J. Perera and M. S. Strano, *Nano Lett.*, 2010, **10**, 398–405.
24 M. H. Rümmeli, C. G. Rocha, F. Ortmann, I. Ibrahim, H. Sevincli, F. Börrnert, J. Kunstmann, A. Bachmatiuk, M. Pötschke, M. Shiraishi, M. Meyyappan, B. Büchner, S. Roche and G. Cuniberti, *Adv. Mater.*, 2011, **23**, 4471–4490.
25 S. Park and R. S. Ruoff, *Nat. Nanotechnol.*, 2009, **4**, 217–224.
26 D. Chen, L. Tang and J. Li, *Chem. Soc. Rev.*, 2010, **39**, 3157–3180.
27 (*a*) M. Lotya, P. J. King, U. Khan, S. De and J. N. Coleman, *ACS Nano*, 2010, **4**, 3155–3162; (*b*) A. A. Green and M. C. Hersam, *Nano Lett.*, 2009, **9**, 4031–4036.
28 Web-Resource, 28 Feb 2012: www.nanointegris.com.
29 (*a*) Y. Hernandez, V. Nicolosi, M. Lotya, F. M. Blighe, Z. Sun, S. De, I. T. McGovern, B. Holland, M. Byrne, Y. K. Gun'Ko, J. J. Boland, P. Niraj, G. Duesberg, S. Krishnamurthy, R. Goodhue, J. Hutchison, V. Scardaci, A. C. Ferrari and J. N. Coleman, *Nat. Nanotechnol.*, 2008, **3**, 563–568; (*b*) U. Khan, A. O'Neill, M. Lotya, S. De and J. N. Coleman, *Small*, 2010, **6**, 864–871.
30 (*a*) A. Dato, V. Radmilovic, Z. Lee, J. Phillips and M. Frenklach, *Nano Lett.*, 2008, **8**, 2012–2016; (*b*) A. Dato, Z. Lee, K.-J. Jeon, R. Erni, V. Radmilovic, T. J. Richardson and M. Frenklach, *Chem. Commun.*, 2009, 6095–6097.
31 Web-Resource, 28 Feb 2012: www.graphene-supermarket.com.
32 W. S. Hummers and R. E. Offeman, *J. Am. Chem. Soc.*, 1958, **80**, 1339–1339.
33 Y. Shao, J. Wang, H. Wu, J. Liu, I. A. Aksay and Y. Lin, *Electroanalysis (N. Y.)*, 2010, **22**, 1027–1036.
34 D. A. C. Brownson and C. E. Banks, *Phys. Chem. Chem. Phys.*, 2012, **14**, 8264–8281.
35 A. Reina, X. Jia, J. Ho, D. Nezich, H. Son, V. Bulovic, M. S. Dresselhaus and J. Kong, *Nano Lett.*, 2009, **9**, 30–35.
36 X. Li, W. Cai, L. Colombo and R. S. Ruoff, *Nano Lett.*, 2009, **9**, 4268–4272.
37 X. Li, C. W. Magnuson, A. Venugopal, R. M. Tromp, J. B. Hannon, E. M. Vogel, L. Colombo and R. S. Ruoff, *J. Am. Chem. Soc.*, 2011, **133**, 2816–2819.
38 (*a*) C. P. Jones, K. Jurkschat, A. Crossley and C. E. Banks, *J. Iran. Chem. Soc.*, 2008, **5**, 279–285; (*b*) C. E. Banks, A. Crossley, C. Salter, S. J. Wilkins and R. G. Compton, *Angew. Chem., Int. Ed.*, 2006, **45**, 2533–2537.
39 X. Li, Y. Zhu, W. Cai, M. Borysiak, B. Han, D. Chen, R. D. Piner, L. Colombo and R. S. Ruoff, *Nano Lett.*, 2009, **9**, 4359–4363.
40 A. J. Bard and L. R. Faulkner, *Electrochemical methods: fundamentals and applications*, John Wiley & Sons, Inc., United States of America, 2nd edn, 2001.
41 H. Matsuda and Y. Ayabe, *Z. Elektrochem.*, 1955, **59**, 494–503.
42 R. S. Nicholson, *Anal. Chem.*, 1965, **37**, 1351–1355.
43 T. J. Davies, C. E. Banks and R. G. Compton, *J. Solid State Electrochem.*, 2005, **9**, 797–808.
44 (*a*) R. G. Compton, C. E. Banks, *Understanding Voltammetry*, World Scientific, Singapore, 2007; (*b*) J. Wang, *Analytical Electrochemistry*, Wiley-VCH, New York, 2nd edn, 2000; (*c*) A. C. Fisher, *Electrode Dynamics*, Oxford University Press, Oxford, 1996.
45 C. E. Banks, T. J. Davies, G. G. Wildgoose and R. G. Compton, *Chem. Commun.*, 2005, 829–841.
46 K. R. Ward, N. S. Lawrence, R. S. Hartshorne and R. G. Compton, *Phys. Chem. Chem. Phys.*, 2012, **14**, 7264–7275.
47 W. Li, C. Tan, M. A. Lowe, H. D. Abruna and D. C. Ralph, *ACS Nano*, 2011, **5**, 2264–2270.
48 A. T. Valota, I. A. Kinloch, K. S. Novoselov, C. Casiraghi, A. Eckmann, E. W. Hill and R. A. W. Dryfe, *ACS Nano*, 2011, **5**, 8809–8815.
49 F. Banhart, J. Kotakoski and A. V. Krasheninnikov, *ACS Nano*, 2011, **5**, 26–41.
50 R. S. Robinson, K. Sternitzke, M. T. McDermott and R. L. McCreery, *J. Electrochem. Soc.*, 1991, **138**, 2412–2418.
51 D. A. C. Brownson, L. J. Munro, D. K. Kampouris and C. E. Banks, *RSC Adv.*, 2011, **1**, 978–988.
52 P. Chen and R. L. McCreery, *Anal. Chem.*, 1996, **68**, 3958–3965.
53 A. G. Güell, N. Ebejer, M. E. Snowden, J. V. Macpherson and P. R. Unwin, *J. Am. Chem. Soc.*, 2012, **134**, 7258–7261.
54 D. K. Kampouris and C. E. Banks, *Chem. Commun.*, 2010, **46**, 8986–8988.
55 C. X. Lim, H. Y. Hoh, P. K. Ang and K. P. Loh, *Anal. Chem.*, 2010, **82**, 7387–7393.
56 (*a*) X. Ji, C. E. Banks, A. Crossley and R. G. Compton, *ChemPhysChem*, 2006, **7**, 1337–1344; (*b*) A. Chou, T. Böcking, N. K. Singh and J. J. Gooding, *Chem. Commun.*, 2005, 842–844; (*c*) L. Tang, Y. Wang, Y. Li, H. Feng, J. Lu and J. Li, *Adv. Funct. Mater.*, 2009, **19**, 2782–2789; (*d*) S. P. Kumar, R. Manjunatha, C. Nethravathi, G. S. Suresh, M. Rajamathi and T. V. Venkatesha, *Electroanalysis (N. Y.)*, 2011, **23**, 842–849; (*e*) J. Premkumar and S. B. Khoo, *J. Electroanal. Chem.*, 2005, **576**, 105–112.
57 (*a*) G. P. Keeley, A. O'Neill, N. McEvoy, N. Peltekis, J. N. Coleman and G. S. Duesberg, *J. Mater. Chem.*, 2010, **20**, 7864–7869; (*b*) G. P. Keeley, A. O'Neill, M. Holzinger, S. Cosnier, J. N. Coleman and G. S. Duesberg, *Phys. Chem. Chem. Phys.*, 2011, **13**, 7747–7750.
58 A. Ambrosi, A. Bonanni and M. Pumera, *Nanoscale*, 2011, **3**, 2256–2260.
59 C. Tan, J. Rodriguez-Lopez, J. J. Parks, N. L. Ritzert, D. C. Ralph and H. D. Abruna, *ACS Nano*, 2012, **6**, 3070–3079.
60 H. L. Poh, F. Sanek, A. Ambrosi, G. Zhao, Z. Sofer and M. Pumera, *Nanoscale*, 2012, **4**, 3515–3522.
61 (*a*) B. Guo, L. Fang, B. Zhang and J. R. Gong, *Insciences J.*, 2011, **1**, 80–89; (*b*) X. Huang, X. Qi, F. Boey and H. Zhang, *Chem. Soc. Rev.*, 2012, **41**, 666–686.
62 (*a*) D. A. C. Brownson, J. P. Metters, D. K. Kampouris and C. E. Banks, *Electroanalysis (N. Y.)*, 2011, **23**, 894–899; (*b*) D. A. C. Brownson and C. E. Banks, *Electrochem. Commun.*, 2011, **13**, 111–113; (*c*) D. A. C. Brownson and C. E. Banks, *Analyst*, 2011, **136**, 2084–2089; (*d*) D. A. C. Brownson and C. E. Banks, *Chem. Commun.*, 2012, **48**, 1425–1427.
63 (*a*) S. Y. Chee and M. Pumera, *Analyst*, 2012, **137**, 2039–2041; (*b*) A. Ambrosi, S. Y. Chee, B. Khezri, R. D. Webster, Z. Sofer and M. Pumera, *Angew. Chem., Int. Ed.*, 2012, **51**, 500–503.
64 P. M. Hallam and C. E. Banks, *Phys. Chem. Chem. Phys.*, 2011, **13**, 1210–1213.
65 (*a*) I. Streeter, G. G. Wildgoose, L. Shao and R. G. Compton, *Sens. Actuators, B*, 2008, **133**, 462–466; (*b*) M. J. Sims, N. V. Rees, E. J. F. Dickinson and R. G. Compton, *Sens. Actuators, B*, 2010, **144**, 153–158; (*c*) M. C. Henstridge, E. J. F. Dickinson, M. Aslanoglu, C. Batchelor-McAuley and R. G. Compton, *Sens. Actuators, B*, 2010, **145**, 417–427.
66 S.-X. Guo, S.-F. Zhao, A. M. Bond and J. Zhang, *Langmuir*, 2012, **28**, 5275–5285.
67 (*a*) D. R. Dreyer, S. Park, C. W. Bielawski and R. S. Rouff, *Chem. Soc. Rev.*, 2010, **39**, 228–240; (*b*) L. J. Cote, J. Kim, V. C. Tung, J. Luo, F. Kim and J. Huang, *Pure Appl. Chem.*, 2011, **83**, 95–110.
68 D. A. C. Brownson, A. C. Lacombe, M. Gomez-Mingot and C. E. Banks, *RSC Adv.*, 2012, **2**, 665–668.
69 M. Zhou, Y. Wang, Y. Zhai, J. Zhai, W. Ren, F. Wang and S. Dong, *Chem.–Eur. J.*, 2009, **15**, 6116–6120.
70 (*a*) D. A. C. Brownson and C. E. Banks, *Phys. Chem. Chem. Phys.*, 2011, **13**, 15825–15828; (*b*) D. A. C. Brownson,

M. Gomez-Mingot and C. E. Banks, *Phys. Chem. Chem. Phys.*, 2011, **13**, 20284–20288.
71 (*a*) A. N. Obraztsov, E. A. Obraztsova, A. V. Tyurnina and A. A. Zolotukhin, *Carbon*, 2007, **45**, 2017–2021; (*b*) K. S. Kim, Y. Zhao, H. Jang, S. Y. Lee, J. M. Kim, K. S. Kim, J.-H. Ahn, P. Kim, J.-Y. Choi and B. H. Hong, *Nature*, 2009, **457**, 706–710.
72 A. Guermoune, T. Chari, F. Popescu, S. S. Sabri, J. Guillemette, H. S. Skulason, T. Szkopek and M. Siaj, *Carbon*, 2011, **49**, 4204–4210.
73 D. A. C. Brownson, D. K. Kampouris and C. E. Banks, *J. Power Sources*, 2011, **196**, 4873–4885.
74 (*a*) K. R. Ratinac, W. Yang, J. J. Gooding, P. Thordarson and F. Braet, *Electroanalysis (N. Y.)*, 2011, **23**, 803–826; (*b*) T. Gan and S. Hu, *Microchim. Acta*, 2011, **175**, 1–19.
75 (*a*) B. Ntsendwana, B. B. Mamba, S. Sampath and O. A. Arotiba, *Int. J. Electrochem. Sci.*, 2012, **7**, 3501–3512; (*b*) J. Li, S. Guo, Y. Zhai and E. Wang, *Anal. Chim. Acta*, 2009, **649**, 196–201; (*c*) Y.-R. Kim, S. Bong, Y.-J. Kang, Y. Yang, R. K. Mahajan, J. S. Kim and H. Kim, *Biosens. Bioelectron.*, 2010, **25**, 2366–2369; (*d*) Y. Wang, Y. Wan and D. Zhang, *Electrochem. Commun.*, 2010, **12**, 187–190; (*e*) A. Navaee, A. Salimi and H. Teymourian, *Biosens. Bioelectron.*, 2012, **31**, 205–211; (*f*) J. Peng, C. Hou and X. Hu, *Int. J. Electrochem. Sci.*, 2012, **7**, 1724–1733.
76 W.-J. Lin, C.-S. Liao, J.-H. Jhang and Y.-C. Tsai, *Electrochem. Commun.*, 2009, **11**, 2153–2156.
77 Y. Wang, D. Zhang and J. Wu, *J. Electroanal. Chem.*, 2012, **664**, 111–116.
78 X. Kang, J. Wang, H. Wu, J. Liu, I. A. Aksay and Y. Lin, *Talanta*, 2010, **81**, 754–759.
79 D. A. C. Brownson, C. W. Foster and C. E. Banks, *Analyst*, 2012, **137**, 1815–1823.
80 D. A. C. Brownson, A. C. Lacombe, D. K. Kampouris and C. E. Banks, *Analyst*, 2012, **137**, 420–423.
81 (*a*) M. S. Goh and M. Pumera, *Anal. Chem.*, 2010, **82**, 8367–8370; (*b*) M. S. Goh and M. Pumera, *Anal. Bioanal. Chem.*, 2011, **399**, 127–131.
82 D. A. C. Brownson, R. V. Gorbachev, S. J. Haigh and C. E. Banks, *Analyst*, 2012, **137**, 833–839.
83 (*a*) L. M. Goncalves, C. Batchelor-McAuley, A. A. Barros and R. G. Compton, *J. Phys. Chem. C*, 2010, **114**, 14213–14219; (*b*) Q. Li, C. Batchelor-McAuley and R. G. Compton, *J. Phys. Chem. B*, 2010, **114**, 7423–7428.
84 E. P. Randviir and C. E. Banks, *RSC Adv.*, 2012, **2**, 5800–5805.
85 (*a*) M. S. Goh, A. Bonanni, A. Ambrosi, Z. Sofer and M. Pumera, *Analyst*, 2011, **136**, 4738–4744; (*b*) M. S. Goh and M. Pumera, *Anal. Chim. Acta*, 2012, **711**, 29–31.
86 (*a*) S. Wu, X. Lan, F. Huang, Z. Luo, H. Ju, C. Meng and C. Duan, *Biosens. Bioelectron.*, 2012, **32**, 293–296; (*b*) K. J. Huang, D. J. Niu, J. Y. Sun, C. H. Han, Z. W. Wu, Y. L. Li and X. Q. Xiong, *Colloids Surf., B: Biointerfaces*, 2011, **82**, 543–549; (*c*) N. G. Shang, P. Papakonstantinou, M. McMullan, M. Chu, A. Stamboulis, A. Potenza, S. S. Dhesi and H. Marchetto, *Adv. Funct. Mater.*, 2008, **18**, 3506–3514.
87 (*a*) B. Jiang, M. Wang, Y. Chen, J. Xie and Y. Xiang, *Biosens. Bioelectron.*, 2012, **32**, 305–308; (*b*) Y. Fang, S. Guo, C. Zhu, Y. Zhai and E. Wang, *Langmuir*, 2010, **26**, 11277–11282; (*c*) Y. Wei, C. Gao, F.-L. Meng, H.-H. Li, L. Wang, J.-H. Liu and X.-J. Huang, *J. Phys. Chem. C*, 2012, **116**, 1034–1041; (*d*) H. Li, J. Chen, S. Han, W. Niu, X. Liu and G. Xu, *Talanta*, 2009, **79**, 165–170; (*e*) S. Guo, D. Wen, Y. Zhai, S. Dong and E. Wang, *ACS Nano*, 2010, **4**, 3959–3968.
88 Z.-H. Sheng, X.-Q. Zheng, J.-Y. Xu, W.-J. Bao, F.-B. Wang and X.-H. Xia, *Biosens. Bioelectron.*, 2012, **34**, 125–131.
89 X. Kang, J. Wang, H. Wu, I. A. Aksay, J. Liu and Y. Lin, *Biosens. Bioelectron.*, 2009, **25**, 901–905.
90 S. L. Candelaria, Y. Shao, W. Zhou, X. Li, J. Xiao, J.-G. Zhang, Y. Wang, J. Liu, J. Li and G. Cao, *Nano Energy*, 2012, **1**, 195–220.
91 (*a*) Y. Sun, Q. Wu and G. Shi, *Energy Environ. Sci.*, 2011, **4**, 1113–1132; (*b*) L. Grande, V. T. Chundi, D. Wei, C. Bower, P. Andrew and T. Ryhanen, *Particuology*, 2012, **10**, 1–8; (*c*) A. Kumar, C. S. Rout and T. S. Fisher, *J. Nano Energy Power Res.*, 2011, **1**, 16–32; (*d*) L. L. Zhang, R. Zhou and X. S. Zhao, *J. Mater. Chem.*, 2010, **20**, 5983–5992.
92 M. D. Stoller, S. Park, Y. Zhu, J. An and R. S. Ruoff, *Nano Lett.*, 2008, **8**, 3498–3502.
93 J. R. Miller, R. A. Outlaw and B. C. Holloway, *Electrochim. Acta*, 2011, **56**, 10443–10449.
94 X. Du, P. Guo, H. Song and X. Chen, *Electrochim. Acta*, 2010, **55**, 4812–4819.
95 Y. Wang, Z. Shi, Y. Huang, Y. Ma, C. Wang, M. Chen and Y. Chen, *J. Phys. Chem. C*, 2009, **113**, 13103–13107.
96 M. S. Goh and M. Pumera, *Electrochem. Commun.*, 2010, **12**, 1375–1377.
97 K. Zhang, L. Mao, L. L. Zhang, H. S. O. Chan, S. Zhao and J. Wu, *J. Mater. Chem.*, 2011, **21**, 7302–7307.
98 D. Qu, *J. Power Sources*, 2002, **109**, 403–411.
99 B. Zhao, P. Liu, Y. Jiang, D. Pan, H. Tao, J. Song, T. Fang and W. Xu, *J. Power Sources*, 2012, **198**, 423–427.
100 (*a*) K. Zhang, L. L. Zhang, X. S. Zhao and J. Wu, *Chem. Mater.*, 2010, **22**, 1392–1401; (*b*) Y. Chen, X. Zhang, P. Yu and Y. Ma, *J. Power Sources*, 2010, **195**, 3031–3035; (*c*) K.-S. Kim, I.-J. Kim and S.-J. Park, *Synth. Met.*, 2010, **160**, 2355–2360; (*d*) W. Shi, J. Zhu, D. H. Sim, Y. Y. Tay, Z. Lu, X. Zhang, Y. Sharma, M. Srinivasan, H. Zhang, H. H. Hng and Q. Yan, *J. Mater. Chem.*, 2011, **21**, 3422–3427; (*e*) H. Wang, H. S. Casalongue, Y. Liang and H. Dai, *J. Am. Chem. Soc.*, 2010, **132**, 7472–7477.
101 J. Yan, T. Wei, B. Shao, Z. Fan, W. Qian, M. Zhang and F. Wei, *Carbon*, 2010, **48**, 487–493.
102 J. Yan, T. Wei, Z. Fan, W. Qian, M. Zhang, X. Shen and F. Wei, *J. Power Sources*, 2010, **195**, 3041–3045.
103 M. Liang and L. Zhi, *J. Mater. Chem.*, 2009, **19**, 5871–5878.
104 P. Lian, X. Zhu, S. Liang, Z. Li, W. Yang and H. Wang, *Electrochim. Acta*, 2010, **55**, 3909–3914.
105 D. Pan, S. Wang, B. Zhao, M. Wu, H. Zhang, Y. Wang and Z. Jiao, *Chem. Mater.*, 2009, **21**, 3136–3142.
106 T. Bhardwaj, A. Antic, B. Pavan, V. Barone and B. D. Fahlman, *J. Am. Chem. Soc.*, 2010, **132**, 12556–12558.
107 (*a*) E. J. Yoo, J. Kim, E. Hosono, H.-S. Zhou, T. Kudo and I. Honma, *Nano Lett.*, 2008, **8**, 2277–2282; (*b*) T. Takamura, K. Endo, L. Fu, Y. Wu, K. J. Lee and T. Matsumoto, *Electrochim. Acta*, 2007, **53**, 1055–1061.
108 (*a*) S.-M. Paek, E. Yoo and I. Honma, *Nano Lett.*, 2009, **9**, 72–75; (*b*) X. Wang, X. Zhou, K. Yao, J. Zhang and Z. Liu, *Carbon*, 2011, **49**, 133–139; (*c*) H. Wang, L.-F. Cui, Y. Yang, H. S. Casalongue, J. T. Robinson, Y. Liang, Y. Cui and H. Dai, *J. Am. Chem. Soc.*, 2010, **132**, 13978–13980; (*d*) Y. Ding, Y. Jiang, F. Xu, J. Yin, H. Ren, Q. Zhuo, Z. Long and P. Zhang, *Electrochem. Commun.*, 2010, **12**, 10–13.
109 G. Zhou, D.-W. Wang, F. Li, L. Zhang, N. Li, Z.-S. Wu, L. Wen, G. Q. Lu and H.-M. Cheng, *Chem. Mater.*, 2010, **22**, 5306–5313.
110 L. Qu, Y. Liu, J.-B. Baek and L. Dai, *ACS Nano*, 2010, **4**, 1321–1326.
111 (*a*) Y. Zhang, G. Mo, X. Li, W. Zhang, J. Zhang, J. Ye, X. Huang and C. Yu, *J. Power Sources*, 2011, **196**, 5402–5407; (*b*) L. Xiao, J. Damien, J. Luo, H. D. Jang, J. Huang and Z. He, *J. Power Sources*, 2012, **208**, 187–192.
112 C. Liu, S. Alwarappan, Z. Chen, X. Kong and C.-Z. Li, *Biosens. Bioelectron.*, 2010, **25**, 1829–1833.
113 (*a*) R. I. Jafri, N. Rajalakshmi and S. Ramaprabhu, *J. Mater. Chem.*, 2010, **20**, 7114–7117; (*b*) J. Wu, Y. Wang, D. Zhang and B. Hou, *J. Power Sources*, 2011, **196**, 1141–1144.
114 Y. Xin, J.-G. Liu, Y. Zhou, W. Liu, J. Gao, Y. Xie, Y. Yin and Z. Zou, *J. Power Sources*, 2011, **196**, 1012–1018.
115 N. Shang, P. Papakonstantinou, P. Wang and S. R. P. Silva, *J. Phys. Chem. C*, 2010, **114**, 15837–15841.
116 N. Soin, S. S. Roy, T. H. Lim and J. A. D. McLaughlin, *Mater. Chem. Phys.*, 2011, **129**, 1051–1057.
117 (*a*) L. Gomez-Du-Arco, Y. Zhang, C. W. Schlenker, K. Ryu, M. E. Thompson and C. Zhou, *ACS Nano*, 2010, **4**, 2865–2873; (*b*) Y.-Y. Choi, S. J. Kang, H.-K. Kim, W. M. Choi and S.-I. Na, *Sol. Energy Mater. Sol. Cells*, 2012, **96**, 281–285.
118 H. Bi, F. Huang, J. Liang, X. Xie and M. Jiang, *Adv. Mater.*, 2011, **23**, 3202–3206.
119 J. C. Meyer, C. Kisielowski, R. Erni, M. D. Rossell, M. F. Crommie and A. Zettl, *Nano Lett.*, 2008, **8**, 3582–3586.
120 M. M. Ugeda, I. Brihuega, F. Guinea and J. M. Gomez-Rodriguez, *Phys. Rev. Lett.*, 2010, **104**, 096804.

 